UC San Diego
UC San Diego Electronic Theses and Dissertations

Title

Comparison of BC and BrC Absorption from AERONET and In Situ Apportionment at Wintertime Fresno

Permalink

https://escholarship.org/uc/item/9zg7b35f

Author

Chen, Sijie

Publication Date

2018

Peer reviewed|Thesis/dissertation

UNIVERSITY OF CALIFORNIA SAN DIEGO

Comparison of BC and BrC Absorption from AERONET and In Situ Apportionment at

Wintertime Fresno

A Thesis submitted in partial satisfaction of the requirements for the degree Master

of Science

in

Earth Science

by

Sijie Chen

Committee in charge:

    Lynn Russell, Chair
    Amato Evan
    Dan Lubin

2018

Signature Page

The Thesis of Sijie Chen is approved, and it is acceptable in quality and form for

publication on microfilm and electronically:

_____

_____

_____

Chair

University of California San Diego 2018

Table of Contents

List of Figures

List of Tables

Acknowledgements

I would like to acknowledge Professor Lynn Russell for her support as the chair of my committee. Through the 2-year-research and multiple drafts, her guidance has proved to be invaluable.

Abstract of the Thesis

Comparison of BC and BrC Absorption from AERONET and In Situ Apportionment at

Wintertime Fresno

by

Sijie Chen

Master of Science in Earth Science

University of California San Diego, 2018

Professor Lynn Russell, Chair

The significant radiative impacts of black carbon (BC) and brown carbon (BrC)

have been increasingly recognized but remain highly uncertain. The Aerosol Robotic

Network (AERONET) provides measurements of aerosol absorption optical depths

(AAOD) and other parameters which could be used to estimate BC and BrC absorption

across its global network, but the uncertainty of the apportionment method is not well

understood. Surface measurements of aerosol optical properties were collected from January 13 to February 10, 2013, and from December 25, 2014, to January 13, 2015, at Fresno, California. This work compares the BC and BrC fractions from AERONET measurements apportioned by the absorption angstrom exponent (AAE) method and from the in situ measurements apportioned by the mass absorption coefficients (MAC) and thermodenuder (TD) method and scaled to planetary boundary layer height (PBLH). During the 2013 campaign, the AERONET apportionment shows that BC contributes 67% and BrC contributes 33% of the absorption at 440 nm while the in situ apportionment shows that BC contributes 89% and BrC contributes 11% of the absorption at 405 nm. During the 2014 campaign, the fraction is 72% BC and 28% BrC from the AERONET apportionment, and 68% BC and 32% BrC from the in situ apportionment. The comparisons show stronger correlations between AERONET and in situ measurements in 2014. These results show that the estimates of BC and BrC absorption from AERONET measurements using the AERONET-AAE method have good agreement with in situ estimates when the surface measurements are representative of the column properties.

Section 1 Introduction

1.1 The importance of black carbon and brown carbon to climate forcing

Black carbon (BC) and absorbing organic carbon (OC), which is known as brown carbon (BrC), can significantly impact the climate because they have been suggested to have substantial positive radiative forcing [*Bond et al.*, 2013; *Corrigan et al.*, 2008]. BC and BrC are both carbonaceous components in the atmospheric aerosols, which play various roles in the climate system. Defined as a collection of solid or liquid particles suspended in the air, aerosols have been found to have adverse effects on air quality and human health by elevating the concentration of particulate matter (PM) [*Pope and Dockery*, 2006; *Watson*, 2002]. However, aerosols particles also receive lot of scientific attention for their critical roles in the regulation of the amount of solar radiation absorbed by the earth system.

Due to the mixed nature of aerosols and the complicated processes they undergo, a separate analysis for each chemical component and each process is necessary to gain a sophisticated understanding of aerosol climate forcing. The most recent IPCC report summarizes aerosol effective radiative forcing (ERF) as the sum of irradiance changes from aerosol-radiation interactions (ARI) and aerosol-cloud interactions (ACI). The ARI includes the direct effect and the semi-direct effect from 7 different aerosol components. The direct effect is the effect in which aerosols scatter and absorb shortwave and longwave radiation, thereby altering the radiative balance of the Earth-atmosphere system. The semi-direct effect is the absorption of solar

1

radiation by absorbing aerosols, which changes the static stability and the surface energy budget and may lead to an evaporation of cloud particles. The ACI includes the cloud albedo effect and the lifetime effect (subdivided into cloud lifetime effect, thermodynamic effect and glaciation indirect effect). The total ERF due to aerosols (ARI+ACI, excluding the effect of absorbing aerosol on snow and ice) is calculated to be -0.9 (-1.9 to -0.1) Wm^{-2} [*Stocker and Intergovernmental Panel on Climate Change. Working Group I.*]. While the total effect is found to be negative, certain components are found to be positive (BC: 0.4 (+0.05 to +0.8) Wm^{-2}) or potentially positive (primary and secondary organic aerosol (POA and SOA): -0.12 (-0.4 to +0.1) Wm^{-2}, biomass burning emissions: +0.0 (-0.2 to +0.2) Wm^{-2}, and mineral dust: -0.1 (-0.3 to +0.1) Wm^{-2}) [*Stocker and Intergovernmental Panel on Climate Change. Working Group I.*]. Although recent work suggests that the IPCC estimation could have been biased high, the wide range of these potential warming agents indicate more knowledge is needed to allow more precise estimation [*X Wang et al.*, 2014c].

These principal absorbing components, BC, BrC and dust, are known as light absorbing aerosols, referring to their ability to absorb light and transform electromagnetic energy into thermal energy [*Moosmuller et al.*, 2009]. While dust does not share the mainly anthropogenic combustion origin of the others, BC and BrC are often co-emitted and mixed externally and internally, therefore adding to the difficulty of characterization of their properties [*Andreae and Gelencser*, 2006]. With limited understanding of their properties and interactions, BC and BrC represent one of the largest sources of uncertainty in future climate change [*Bond et al.*, 2013; *Myhre et al.*,

2013; *X Wang et al.*, 2014c].

1.2 Current knowledge of BC and BrC

BC is summarized as a black, blackish or brown substance formed by combustion, present in the atmosphere as fine particles. It has been used largely synonymously with soot and elemental carbon (EC) due to their blackness, combustion origin, and thermally refractory nature [*Andreae and Gelencser*, 2006; *Chow et al.*, 1993; *Matthes*, 2008]. Since definitions are based largely on origin and measurement type rather than on material properties, studies have suggested that assuming BC is equal to EC and/or soot carbon is over-simplified and proposed other terminology [*Desyaterik et al.*, 2013; *Shen et al.*, 2013; *Singh et al.*, 2014]. There is not yet an agreement on this issue. In this work, BC and comparable constituents in other studies are referred as BC.

In the past decade or so, BC has been identified as the most important absorber in visible bands [*Ramanathan and Carmichael*, 2008; *Xu et al.*, 2009]. Being able to strongly absorb the solar radiation across the visible spectrum, the direct radiative forcing (DRF) of BC is estimated to range from 0.17 to 1.48 Wm^{-2} [*Bond et al.*, 2013]. This estimate makes BC the second largest anthropogenic warming agent, less than only carbon dioxide [*IPCC*, 2013]. However, BC has a much shorter atmospheric lifetime, typically modelled as close to 1 week, compared to that of greenhouse gases (years to decades) [*Hodnebrog et al.*, 2016]. The shorter lifetime suggests that atmospheric responses to changes in BC concentration could be rapid. It also

suggests the properties of BC can vary with specific source, amount, or mechanism, in addition to other local and temporal factors such as meteorological conditions.

In comparison, the properties of BrC are poorly understood and the definition of BrC, as light absorbing organic matter (OM) that is not soot carbon, is frequently considered imprecise and sometimes lead to confusion in BrC studies [*Andreae and Gelencser*, 2006]. In the early studies, OC has been treated as non-absorbing and therefore only has a scattering effect by climate models. Recent studies found that certain components of OC are absorbing, especially at short wavelengths, and that the scale of absorption might be comparable to the BC absorption [*Andreae and Gelencser*, 2006; *Hoffer et al.*, 2006; *Kirchstetter et al.*, 2004]. Global simulations show that BrC accounts for an average 21% of the global mean surface OC concentration[*Jo et al.*, 2016]. It suggests BrC is not, or is not always, the largest subclass of OC, which means that measurements targeted at OC could have fundamental differences from measurements that targeted specifically at BrC. On the other hand, some studies have focused on biomass burning events, such as forest or savanna fires, to characterize BrC [*Kirchstetter et al.*, 2004; *D. A. Lack et al.*, 2012]. Although biomass burning is identified as the most important source of BrC, there are other production mechanisms, such as fossil fuel combustion, biogenic aerosols and soil humic matters, as well as secondary formation from various precursors [*D. A. Lack and Langridge*, 2013; *Yang et al.*, 2009; *Q Zhang et al.*, 2011a]. There has been further division of BrC into water-soluble organic carbon (WSOC) and water-insoluble organic carbon (WIOC) [*Sullivan and Weber*, 2006]. There is also division based on chemical speciation into humic-like

4

substances (HULIS) and tar balls [*Chakrabarty et al.*, 2010; *Cheng et al.*, 2016; *Hoffer et al.*, 2016]. In this work, BrC and comparable constituents in other studies are referred as BrC, noting that differences caused by definition might be significant.

The global estimation of the DRF of BrC is limited by the knowledge of the sources, optical properties, and chemical transformations. In addition, the lifetime of BrC also adds to large uncertainties. The decrease with photochemical aging with a lifetime from 9 hours to 1 day is reported from field campaigns [*Forrister et al.*, 2015; *Lee et al.*, 2014; *Zhao et al.*, 2015]. The shorter lifetime suggests that BrC might have stronger regional and temporal dependence than BC. Studies estimate the DRF of BrC to range from +0.1 to +0.6 Wm^{-2} by modelling its contribution as 20 to 40% of total carbonaceous aerosol absorption [*C. E. Chung et al.*, 2012b; *Feng et al.*, 2013; *Jo et al.*, 2016; *Lin et al.*, 2014; *Rawad Saleh et al.*, 2014; *Q Q Wang et al.*, 2014a]. However, the methods used in each study to measure BrC need to be discussed.

1.3 Apportionment methods and associate parameters

Studies of BC and BrC properties depends on direct measurements of corresponding substances or indirect measurements from apportionment of ambient absorption or total carbonaceous absorption. Based on the distinctive wavelength dependence of BC, BrC and dust, a commonly used method for apportioning total absorption to each absorbing component is known as the AAE method [*Bahadur et al.*, 2012; *Bond and Bergstrom*, 2006; *Cheng et al.*, 2011; *C. E. Chung et al.*, 2012b]. The name comes from absorption angstrom exponent (AAE), which is a crucial parameter

for the light absorption property known as wavelength dependence:

$$AAE = -\frac{\ln\left(\frac{abs(\lambda 1)}{abs(\lambda 2)}\right)}{\ln\left(\frac{\lambda 1}{\lambda 2}\right)} \qquad (1)$$

The $\lambda 1$ and $\lambda 2$ here are two reference wavelengths and $abs(\lambda)$ are the absorption related parameters at the corresponding wavelengths. The AAE method has been developed and widely applied for two reasons: 1) direct measurements are limited, especially for BrC and 2) the AAE method provides efficient apportionment of remote measurements.

Various methods and instruments have been developed to measure ambient optical properties. Filter-based techniques measure aerosols particles that were concentrated and deposited on particle filters. The calculation of light absorption coefficient (b_{abs}) depends on transmission measurements through filters, in addition to information and assumptions about deposited particles [*Moosmuller et al.*, 2009; *Petzold and Schonlinner*, 2004]. In situ techniques evolve based on different principles, such as the temperature increase of particles upon exposure to light (thermal in situ techniques), the optical power and transfer of heat modulated by acoustic frequency (photoacoustic technique), the simultaneous change of the refractive index of the air with the change of temperature (refractive index-based techniques), the thermal emission spectrum of particles heated by high-intensity laser (incandescence-based techniques), and the extinction coefficient (b_{ext}) and the scattering coefficient (extinction-minus-scattering techniques) [*Hariharan*, 2007; *Michelsen*, 2003; *Strawa et al.*, 2003; *Tam*, 1986; *Virkkula et al.*, 2005]. Variations exist due to issues such as

6

filter medium and instrument uncertainties, as well as the potential variability caused by different methodologies [*Davy et al.*, 2017; *X L Zhang et al.*, 2016].

For ambient absorption measurements, several approaches have been used to get direct measurement of BC and BrC. While dust particles have a crustal origin that is relatively easy to distinguish, the extraction of BC and BrC from the absorption, especially the separation of BrC, is a challenge that is subject to considerable uncertainty [*Bond et al.*, 2013; *Kirchstetter et al.*, 2004; *J Liu et al.*, 2013; *J Liu et al.*, 2015a; *X L Zhang et al.*, 2013]. BC and BrC are frequently co-emitted and therefore mixed together internally and externally. One approach for pure BC absorption is using in situ heating at high temperature in a thermodenuder (TD) to remove internally mixed particulate matter, including BrC, by evaporation [*Cappa et al.*, 2012; *D. A. Lack et al.*, 2012; *Nakayama et al.*, 2014; *R. Saleh et al.*, 2013]. This method is known as the TD method. Another approach is to compare measured mass absorption coefficients (MAC) for atmospheric BC to freshly emitted nascent BC, which is assumed to be not mixed with BrC [*Knox et al.*, 2009; *X L Zhang et al.*, 2013]. This method is called the MAC method. Uncertainties in this approach are the result of possible inaccurate or inconsistent measurements and inaccurate assumptions (e.g., incomplete removal of BrC by TD). For BrC, the only method for direct measurements is the extraction of filter samples in water, acetone, or methanol [*Rong Wang et al.*, 2016a]. Most in situ techniques used a more indirect method to calculate BrC from the difference between total absorption and that of BC, which have additional uncertainty since the measurements of BC itself are uncertain [*Bond et al.*, 2013; *Koch et al.*, 2009; *X Wang*

7

et al., 2014c].

In addition to the limitations discussed above, both filter-based and in situ techniques lack the temporal and spatial coverage that is necessary for global estimates. Field campaigns for filter-based or in situ measurement are usually conducted from weeks to months, which means that continuous influence of BC and BrC are hard to determine based on relative short-term evaluations. Furthermore, most studies are concentrated within regions with high emissions (like industrialized urban areas or biomass burning events) [*Andrews et al.*, 2017; *Kirchstetter et al.*, 2004; *D. A. Lack et al.*, 2012]. While these studies might successfully find the prominent characteristics of BC and BrC, they tend to represent higher values from selected area and periods, rather than general values that should be used for global and annual concerns.

The AAE method, on the other hand, is observationally based and uses an empirical approach to determine the fraction of aerosol absorption attributable to each component. It is one of the most basic and widely used methods to study BC and BrC absorption, and it is applicable to remotely sensed measurements [*Bahadur et al.*, 2012; *C. E. Chung et al.*, 2012b; *Russell et al.*, 2010; *X L Zhang et al.*, 2016]. Despite the variations and large uncertainties due to sources, chemical transformations, methodology, and other issues, significantly different AAEs are found for BC and BrC. Reported AAEs for BC are close to 1, but the AAE for BrC is much larger than 1 (Table.1) This indicates BC absorption is less dependent on the wavelength, but BrC absorption is highly dependent on the wavelength. BrC has potentially high

contributions at short wavelengths but it is negligible at longer wavelengths. The AAE method is determined after removing the dust contribution, with the remaining absorption at long wavelength (e.g., 870 nm) considered to be solely from BC. BC absorption at short wavelengths could be calculated based on the AAE of BC, and BrC absorption at short wavelength could be calculated from the difference between total absorption and BC absorption. A typical base case of the AAE method assumes BC absorption to be independent of wavelength (i.e. AAE = 1) and attribute absorption above the predicted BC absorption at short wavelengths to be BrC [*C. E. Chung et al.*, 2012b; *Favez et al.*, 2009; *Fialho et al.*, 2006]. The more complicated AAE method involving consideration of particle size, composition and specific wavelength ranges found that the AAE of BC may not equal to 1 [*Bahadur et al.*, 2012; *Moosmueller et al.*, 2011; *X Wang et al.*, 2016b]. The AAE method treats the AAE of each component as an intrinsic property by composition. This characterization does not incorporate the influence of internal mixing and is confounded by the lack of knowledge of the exact AAE for BC [*Wu et al.*, 2016; *X L Zhang et al.*, 2016]. However, the AAE method is still the basis for apportioning remotely sensed absorption that provides important constraints on modeled vertical aerosol properties [*Andrews et al.*, 2017; *Bond et al.*, 2013; *Koch et al.*, 2009; *X Wang et al.*, 2014c].

1.4 AERONET ground-based remote sensing products

Remote sensing techniques are a fast-evolving area of measuring absorption [*Moosmuller et al.*, 2009]. Scientists have seen enormous potential in understanding

global distributions of absorbing aerosol with the long-term, continuous, and readily available measurements of aerosol optical properties provided through remote sensing network, such as the ground-based Aerosol Robotic Network (AERONET) [*Holben et al.*, 1998; *Holben et al.*, 2001]. AERONET provides crucial products for absorption related column properties such as aerosol optical depth (AOD), aerosol absorption optical depth (AAOD) and column single scattering albedo (SSA). AOD measures the total light extinction in the air column, and the corresponding absorption (AAOD) is calculated as:

$$AAOD = AOD \cdot (1 - SSA) \tag{2}$$

With over 500 sites world-wide, some of which have been operating for nearly 20 years, AERONET provides a possible solution to the limited availability of filter-based and in situ measurements. In addition, the network platform creates a standard for retrieval algorithms and measured wavelengths, which help reduce variation at least in terms of methodology and selected wavelength ranges. At Version 2 of AERONET products, AERONET reports the uncertainty of ±0.01 for AOD and ±0.03 for SSA [*Dubovik et al.*, 2000]. The quality level and uncertainties are further discussed in the following sections. AERONET studies have compared AERONET measurements to corresponding in situ measurements. The validity of AERONET has been tested through direct comparisons with column SSA or AAOD values calculated from airborne in situ measurements [*Corrigan et al.*, 2008; *Esteve et al.*, 2012; *Haywood et al.*, 2003; *Johnson et al.*, 2009; *Leahy et al.*, 2007; *Magi et al.*, 2005; *Mallet et al.*, 2005; *Osborne et al.*, 2008; *Schafer et al.*, 2014]. There are also statistical

assessments that show agreement between AERONET measurements and in situ surface measurements [*Corr et al.*, 2009; *Doran*, 2007; *Dubovik et al.*, 2002; *Mallet et al.*, 2008]. A general good agreement from these comparison studies gives confidence in the AERONET retrievals and leads to the usage of AERONET as a first constraint on modeled aerosol properties. However, there is an estimated average error of 30% in the global representativeness of the locations of AERONET sites because they are close to the high emission sources and because the accuracy of individual retrievals might not be consistent [*Andrews et al.*, 2017; *R. Wang et al.*, 2018]. Therefore, more information is needed for the comparisons between AERONET measurements and in situ measurements, as well as comparison between the AAE method and other apportionment methods.

1.5 Fresno, California

In 2013 and 2014, two field campaigns aimed at obtaining a comprehensive and detailed understanding of the chemical, microphysical, and optical properties of wintertime aerosols within the San Joaquin Valley (SJV) were conducted at Fresno, CA. The SJV is one of the most polluted regions with the highest rates of cardiorespiratory diseases in the USA. Persistent air-quality problems have been associated with high PM concentrations due to anthropogenic missions, topography, and meteorological conditions [*Chow et al.*, 2006]. Studies have shown that the major component of PM in SJV is OM, particularly from residential burning in the severe winter, contributing up to two-thirds of the total mass [*Chow et al.*, 2006; *Chu et al.*,

2004; *Ge et al.*, 2012; *Turkiewicz et al.*, 2006]. The mountainous topography of the SJV traps pollutants and subsequently leads to deterioration of the air quality [*Gorin et al.*, 2006; *Lurmann et al.*, 2006; *Ngo et al.*, 2010]. In addition, the typical cold and high-humidity weather in the wintertime SJV lead to frequent occurrence of regional thick ground fog known as "tule fog". Fog events could enhance aqueous-phase formation of sulfate and SOA, which could contribute to BrC production [*Collett et al.*, 1999; *Ge et al.*, 2012; *Herckes et al.*, 2007]. Therefore, Fresno as one of the most populated cities in SJV, provides an interesting location for studying BC and BrC.

An AERONET-affiliated sun-photometer is maintained by the California Air Resources Board (CARB) near downtown Fresno since 2002. On January 13, 2012, the CARB facility moved 400 m north to the intersection of First and Garland. The AERONET site changed its name to Fresno_2 and has been operating since then. Important parameters for meteorology conditions such as temperature, relative humidity (RH) and visibility have been recorded as part of meteorological aviation reports (METAR) at Fresno Yosemite International Airport (FAT). The two campaigns and local facilities at Fresno thus provide the opportunity to compare in situ measured absorption properties with AERONET measurements closely matched in time and space, as well as testing different apportionment methods for BC and BrC. In addition, assuming emission sources have not changed significantly within 2 years, provides valuable information on how local meteorological conditions could impact absorption measurements and the assumptions used to interpret them.

1.6 The scope of this work

In this work, the question of how accurate AERONET measurements are for estimating BC and BrC absorption is investigated. The use of AERONET measurements to estimate BC and BrC would be beneficial because of the long-term, continuous, and readily available measurements of aerosol absorption across the globally distributed AERONET network. Observations from two winter campaigns in 2013 and 2014 at Fresno were analyzed to better understand the discrepancies between the AERONET column retrievals and the in situ surface-based estimates of column properties. Section 2 presents an overview of AERONET data availability and of the AERONET-AAE method used to apportion AAOD to absorbing components as proposed by Bahadur et al. [2012]. Section 3 summarizes the in situ surface measurements and column estimates made for the two Fresno campaigns. Estimates of column properties are based on the surface measurements of extinction and absorption coefficients and scaled to the simulated planetary boundary layer height (PBLH) from the North American Regional Reanalysis (NARR) for 2013 and from the Weather Research and Forecasting (WRF) model for 2014. The equations and assumptions applied in calculating column properties are presented in Section 3.3. The AERONET-AAE method is modified to represent the low-dust conditions of these campaigns (Section 3.4). The AERONET measurements and the in situ surface-based column estimates for AOD, AAOD, and BC and BrC fractions of AAOD are compared in Section 4. The uncertainties in the calculations and measurements are discussed in Section 4.4.

Section 2 AERONET measurements and the apportionment method

2.1 AERONET measurements availability

AERONET uses a globally-distributed network of automated sun and sky radiometers to provide AOD and AAOD at four wavelengths (440, 675, 870, and 1020 nm) [*Dubovik and King*, 2000; *Holben et al.*, 2001]. The Version 2 AERONET products were introduced based on several major improvements of Version 1, including a revised inversion code, expanded input data, and new criteria for quality assurance. Version 2 includes two levels of data: level 1.5 data have an automatic cloud-screening; level 2.0 data have pre-field and post-field calibrations, manual inspection and quality assurance [*Smirnov et al.*, 2000]. In this work, level 1.5 data are used with the additional quality criteria described below because level 2.0 data are biased toward high aerosol loadings.

One of the major limitations of the level 2.0 data is that SSA retrievals are only available when AOD exceeds 0.4 at 440 nm ($AOD440_{COL} > 0.4$) [*Dubovik et al.*, 2002; *Dubovik and King*, 2000]. However, AeroCom models show that only 5% of days at locations around the world have daily-average $AOD440_{COL}$ that exceeds the 0.4 threshold [*Andrews et al.*, 2017; *Myhre et al.*, 2013]. This limitation means that level 2.0 data represent only a small fraction of days and only those that have high aerosol loadings. This bias is the reason that many studies have chosen to use level 1.5 SSA for their analyses [*Andrews et al.*, 2017; *X Wang et al.*, 2016b].

The drawback of using level 1.5 data is that the measurement uncertainty of

SSA retrievals is higher when $AOD440_{COL}$ is below 0.4. Specifically, the uncertainty for SSA retrievals is ± 0.03 when $AOD440_{COL}$ exceeds 0.4, but the uncertainty could be as large as ± 0.07 when $AOD440_{COL}$ is less than 0.2 due to errors in the surface reflectance [*Dubovik et al.*, 2002]. Andrews et al. [2017] tested the systematic variability of SSA as a function of AOD and their results showed SSA could not be retrieved properly when $AOD440_{COL}$ is below 0.05. In addition, the uncertainty of the AOD measurement (± 0.01) has a significant impact as it is equivalent to 20% of AOD at this low level. Therefore, in this work, a threshold is set at $AOD440_{COL}$ > 0.1, for which the uncertainty for AOD is at maximum 10% of the measurements. Since the chosen range for AOD measurements is subject to larger uncertainty for SSA retrievals, a lognormal distribution is used to obtain a 95% confidence interval based on the assumption that SSAs during each campaign are relatively consistent (i.e. within the range of confidence interval of the mean value). Note that AERONET SSA has a maximum of 1, therefore, it is converted into single scatter co-albedo (SSCA = 1 - SSA) before applying the calculation. The AERONET measurements that fit the quality criteria discussed above are referred to here as "level 1.5M" measurements and are used in the following analysis (Table.2).

A newer version of AERONET, the Version 3 products, has recently become available on the AERONET website. This work uses Version 2 because the key parameters and constraints used for the AERONET-AAE method of Bahadur et al. [2012] are based on Version 2 AERONET products.

2.2 The Bahadur method

The apportionment method of partitioning AERONET AAOD to BC and BrC in this work is based on the AERONET-AAE method constrained by AERONET spectral observations [*Bahadur et al.*, 2012]. This method is referred to as the "Bahadur method" in the following sections. This method is based on the theory of using empirically estimated AAE of BC to derive the absorption due to BrC. It improves on the previous methods because the AAEs used are fit to actual AERONET spectral measurements rather than relying on the laboratory measurements or theoretical values [*Bahadur et al.*, 2012; *C. E. Chung et al.*, 2012b; *Russell et al.*, 2010]. The approach used to obtain the AAEs is to select AERONET sites at which most of the absorption is contributed by dust or by carbonaceous components. These sites are referred to as "dust-dominated" sites and "dust-free" sites in Bahadur et al. [2012]. The AAE of dust, BC and BrC are calculated from the AERONET measurements at corresponding sites. In this work, the term BC is used for what the Bahadur et al. [2012] termed EC; similarly, the term BrC is used for what the Bahadur et al. [2012] termed OC.

The Bahadur method selects dust-dominated and dust-free sites based on the scattering angstrom exponent (SAE) and the ratio of AAEs at separate wavelengths. SAE is calculated from the same equation as AAE (eq.1) but using scattering parameters (sca(λ1) and sca(λ2)) instead of absorption parameters:

$$\text{SAE} = -\frac{\ln\left(\frac{\text{sca}(\lambda 1)}{\text{sca}(\lambda 2)}\right)}{\ln\left(\frac{\lambda 1}{\lambda 2}\right)} \qquad (3)$$

The SAE and AAE values for $\lambda 1$ = 440 nm and $\lambda 2$ = 675 nm are denoted as SAE1 and

AAE1, respectively. The SAE and AAE values for $\lambda 1 = 675$ nm and $\lambda 2 = 870$ nm are denoted as SAE2 and AAE2. Russell et al. [2010] found that the SAE and AAE values associated with aerosols of crustal origin are different from those associated with combustion sources. Sites with SAE1 < 0.5 are considered to be dust-dominated and sites with SAE1 > 1.2 or AAE2/AAE1 > 0.8 are considered to be dust-free. The dust AAE is calculated as the average of all dust-dominated sites to give 2.20 ± 0.50 for AAE1 and 1.15 ± 0.50 for AAE2. The measurements from dust-free sites are separated into two categories, one with weaker spectral dependence because most of the absorption is from BC ("BC-dominated" sites with AAE1 < 0.55 and AAE2 < 0.83), and the other with stronger spectral dependence implying BrC absorption is measurable at these sites. The BC AAE is calculated as the average of all BC-dominated sites to give 0.55 ± 0.24 for AAE1 and 0.85 ± 0.40 for AAE2. The BrC AAE is calculated from the remaining dust-free sites which are assumed to have measurable BrC absorption. The average AAE1 of BrC is calculated to be 4.55 ± 2.01. The AAE2 of BrC is not relevant since that BrC is assumed to not absorb at 870 nm. These values are considered to be constant worldwide for each absorbing component, because they were found to be independent of location, source, and aerosol concentration.

If the AAE values are constant, the Bahadur method is applicable to worldwide AERONET sites with mixed sources. The calculation of apportionment could be expressed as:

$$AAOD\ (\lambda_i)=AAOD_{ref,BC}\left(\frac{\lambda_i}{\lambda_{ref}}\right)^{-AAE_{BC,i}}+AAOD_{ref,BrC}(\frac{\lambda_i}{\lambda_{ref}})^{-AAE_{BrC,i}}$$

$$+AAOD_{ref,dust}(\frac{\lambda_i}{\lambda_{ref}})^{-AAE_{dust,i}}$$

Two assumptions are inherent in equation 4: 1) the AAE values of each absorbing component are intrinsic properties that do not depend on the mixing state; and 2) the measured AAOD values represent a well-mixed sample of these components. With these assumptions, the fractions of AAOD from the three absorbing components at wavelength (λ_i) can be calculated from the AAOD measurements at three wavelengths (440 nm, 675 nm and 870 nm in this work) since equation.4 provides three equations and three unknowns.

The Bahadur method has been applied to a case study of 10 AERONET sites around California. The general agreement with regional emission trends indicates that the Bahadur method provides a reasonable apportionment of each component. However, the AAEs determined from this procedure might not be globally representative. For example, *Bond and Bergstrom* [2006] have argued that the AAEs are strongly size dependent and vary geographically with combustion emissions [*Bond and Bergstrom*, 2006; *X Wang et al.*, 2016b]. Other studies suggest that internal mixing (lensing effect) could lead to absorption enhancement for different mixing states, which might be up to a factor of 1.8 during high pollution events [*Q Y Wang et al.*, 2014b]. Since the AAEs of BC and BrC are determined simultaneously from observations in the dust-free regions, the low end value does not guarantee a complete removal of internal mixing of BrC. Using core-shell Mie theory (Mie-scattering algorithm with core-

shell assumption), the AAE1 of BC could vary from 0.7 (no particles coated) to 0.1 (all particles coated) [*Bahadur et al.*, 2012; *Chul E. Chung et al.*, 2012a; *Gyawali et al.*, 2009]. This range is generally consistent with the uncertainty (0.55 ± 0.24), suggesting that the apportioned BC absorption from the Bahadur method could include some contribution from lensing. Therefore, comparisons of the AERONET apportionment using the Bahadur method to the in situ measurements that were collected close in time and space are necessary to investigate to what extent the AERONET apportionment agrees with surface-based observations.

Section 3 In situ surface measurements and column estimates

3.1 Fresno campaign sites and instrumentation

From January 13 to February 10, 2013, a collection of surface measurements including chemical compositions and optical properties was made at the California Air Resources Board (CARB) Fresno-Garland air monitoring facility (36.7854°, -119.7732°). The site is surrounded by residential and commercial areas, monitoring a mix of rural and urban pollutants, and is approximately 1500 meters to the east of Yosemite FWY-41. In the following sections, this campaign is referred as the 2013 campaign.

PM2.5 dry particle (RH <30%) light extinction at 405 ($b_{ext}405$) and 532 ($b_{ext}532$) nm were measured by a cavity ringdown spectrometer (CRD). PM2.5 dry particle light absorption at 405 ($b_{abs}405$) and 532 ($b_{abs}532$) nm were measured by a photoacoustic spectrometer (PAS). Light extinction and absorption at 870 nm ($b_{ext}870$ and $b_{abs}870$, respectively) were measured by a photoacoustic extinctiometer (PAX). Refractory black carbon (rBC) mass and number size distributions at a size range of 100 to 300 nm were measured by a single particle soot photometer (SP2). The size range was extrapolated to 20 to 1000 nm through bimodal lognormal distribution to estimate the "missing" rBC mass outside of the measurement range. PM1 particle number size distributions (16 - 685 nm) were measured by a scanning mobility particle sizer (SMPS). PM2.5 absorption enhancement at 405 ($E_{abs}405$), 532 ($E_{abs}532$) and 870 ($E_{abs}870$) nm were measured by a thermodenuder (TD). TD was operated at 175 °C

in the first half of its tube and 275 °C in the second half to remove internally and externally mixed BrC. The CRD-PAS, PAX, SP2, and SMPS alternatively sampled either ambient particles or particles that passed through TD on an automated 5 min cycle. The detailed operation, calibration, and results of the CRD-PAS, PAX and SP2 measurements were described by Zhang et al., [2016].

PM1 non refractory submicron particle (NR-PM1) mass and chemical composition were measured by a high resolution time-of-flight aerosol mass spectrometer (HR-ToF-AMS). Measurements include both inorganic (NH_4^+, SO_4^{2-}, NO_3^-, Cl^-) and organic aerosols (OA). A positive matrix factorization (PMF) analysis was performed on the OA mass spectral matrix. Six OA components were resolved, including two types of biomass burning OA (BBOA-1 and BBOA-2), a hydrocarbon-like OA (HOA), a semi-volatile oxygenated OA (SV-OOA), a low volatility oxygenated OA (LV-OOA), and a cooking OA (COA). The good correlation (R^2 = 0.54) between $E_{abs}405$ and the BBOA-to-OA mass concentration ratio together with the observed diurnal behavior indicate that BBOA from nighttime residential wood burning is the most important BrC source over the campaign. Detailed information describing the PMF analysis and absorption analysis can be found in Zhang et al. [2011b], Young et al. [2016] and Zhang et al. [2016].

From December 25, 2014, to January 13, 2015, another campaign was conducted at the University of California Center (36.8101°, -119.7782°). Here this campaign is referred to as the 2014 campaign. Similar measurements were made with CRD-PAS, PAX, SP2, SMPS, TD and HR-ToF-AMS. Details are provided in Betha et

al. [accepted], Chen et al. [in review] and Cappa et al. [unpublished]. In contrast to the previous campaign, four factors of OA were identified by PMF analysis, including a hydrocarbon-like OA (HOA), a biomass burning OA (BBOA), a nitrate-related oxygenated OA (NOOA), and a very oxygenated organic aerosol (VOOA). Both BBOA and NOOA were found to be absorbing, but BBOA is the more efficient absorber with MAC nearly three times higher than NOOA at 405 nm [*Cappa et al.,* unpublished].

In addition, filter samples were collected on pre-scanned Teflon filters (37mm diameter, 1.0 μm pore size). 20 PM1 and 5 PM2.5 filter samples were selected for X-ray fluorescence (XRF) analysis at Chester Laboratories (Chester LabNet, Tigard, Oregon) for measurements of 38 elements heavier than Na. The elements Al, Si, S, K, Ca, Fe, Zn, and Br were above detection limit in at least 80% of the samples and their concentrations are used to quantify dust contributions (Al_2O_3, SiO_2, S, K_2O, $CaCO_3$, Fe_2O_3) and as elemental tracers of biomass burning (K) [Chen et al., unpublished].

Corresponding to the time of both campaigns, AERONET measurements are downloaded from https://aeronet.gsfc.nasa.gov/new_web/index.html. TheFresno_2 (36.7854°, -119.7732°) site is used for both campaigns. The AERONET site is at the same location where 2013 campaign was conducted, except that the AERONET instrument is mounted on the roof of CARB building with at a local elevation of 100.0 m. The location of the 2014 campaign is about 3000 m north of the AERONET site.

The weather information was downloaded from www.wunderground.com/, which is decoded from the METAR record at Fresno Yosemite International Airport (FAT). The scheduled METAR observations took place at the end of each hour. Note

that this source is different from the source of meteorological information used by Zhang et al. [2016] and Pusede et al. [2016].

Figure.1 provides an overview of the comparison between the AERONET AOD440$_{COL}$ and the in situ surfaced-based column estimates of extinction in the PBL at 405 nm (AOD405$_{PBL}$). Because BrC absorption is only significant at short wavelengths, the comparisons in this study focus on the shortest wavelength available from AERONET measurements (440 nm) and in situ measurements (405 nm), unless otherwise specified. Figure.1 shows that after scaling the surface measurements to PBLH, AERONET AOD440$_{COL}$ and in situ AOD405$_{PBL}$ are relatively similar. The assumptions of the estimation process are discussed in the Section 3.3. A high-fog period in 2014 campaign from 7 to 13 January 2015 had slightly warmer temperatures (average temperature 12°C), lower wind speed (0.8 m/s), and persistent fog (indicated by low visibility and high RH) from midnight through morning rush hours [*Chen et al.,* unpublished]. This type of high-fog period is not seen from the 2013 campaign. More than 3000 in situ measurements were collected for each campaign at a 10 min interval, AERONET collects measurements at every 15 min interval, but most measurements are removed by the cloud screening and quality control processes [*Holben et al.*, 1998]. This work focuses on the comparison of AERONET measurements to in situ measurements that correspond in time. The measurements were processed and analyzed using Igor Pro (Wavemetrics). The measurements reported in this work are in local time, which is Pacific standard time (PST) and 8 h earlier than coordinated universal time (UTC).

There was another campaign conducted from July 3, 2015, to July 25, 2015, in Fontana, CA, in order to understand the aerosol chemical and optical properties in the South Coast Air Basin (SoCAB) [*Lee et al.*, 2017; *Chen et al.*, unpublished; *Cappa et al.*, unpublished]. The SoCAB has a very photochemically active environment in the summertime with extensive internal mixing of SOA [*Docherty et al.*, 2008; *Hayes et al.*, 2013]. Unfortunately, the AERONET measurements near Fontana were not available due to an operation problem at the Rogers Dry Lake site and the large elevation difference (~1000m) at Table Mountain site. The sites at CalTech and Santa Monica Colg which are both more than 80 km away have impacts from local emissions at Los Angeles and coastal influences that may not be representative of the Fontana conditions. In addition, the measurements at both sites during the campaign period mostly occurred between 5:00 PM and 7:00 PM (67% of total measurements) with no measurements collected between 10:00 AM and 2:00 PM. These measurements near sunset hours have a low angle of incidence, making them more uncertain. Therefore, a comparison of the AERONET measurements to the in situ measurements was not completed at Fontana in this work.

3.2 In situ apportionment

Light absorption coefficients for BC ($b_{abs,BC}$) and BrC ($b_{abs,BrC}$) were measured in situ using a combination of the MAC and TD methods. The MAC for particles containing BC is dependent on the BC mixing state [*Cappa et al.*, 2012; *Daniel A. Lack et al.*, 2009; *Saathoff et al.*, 2003; *Schnaiter et al.*, 2003; *Schnaiter et al.*, 2005;

Shiraiwa et al., 2010]. When BC is internally mixed with other particulate components, these materials can build up coatings on BC that can act like a lens to focus light, which increases the MAC of BC. This enhancement of light absorption (E_{abs}) is known as the "lensing" effect. The MAC method evaluates the E_{abs} by comparing the observed MAC of BC to the reference value of uncoated BC ($E_{abs} = MAC_{BC}/MAC_{BC,uncoated}$). For the 2013 and 2014 campaigns, instead of using a reference value from the literature, the MAC of uncoated BC is calculated from thermodenuded particles (i.e. using the TD method). The absorption is measured before and after heating in the TD, which is then used to calculates coated and uncoated BC properties [*Cappa et al.*, 2012; *D. A. Lack et al.*, 2012; *Nakayama et al.*, 2014; *R. Saleh et al.*, 2013]. The absorption due to pure, uncoated BC is:

$$b_{abs,BC}=MAC_{BC,uncoated} \cdot [BC] \tag{5}$$

The concentration of BC ([BC]) is calculated from SP2 measurements using a correction for the "missing mass", which accounts for the loss of particles below the lower size limit. For BrC, the absorption is determined by taking the difference between the observed absorption and the estimated absorption of coated BC. This quantity is calculated as:

$$b_{abs,BrC}=b_{abs,obs}-b_{abs,BC,coated}=MAC_{BC,uncoated} \cdot [BC] \cdot E_{abs,mixing}(R_{BC}) \tag{6}$$

The absorption of coated BC is calculated by multiplying the uncoated BC absorption by the mixing-induced enhancement ($E_{abs,mixing}$), which is a function of the coating-to-core mass ratio (R_{BC} = [coating]/[BC]). To determine the $E_{abs,mixing}$ values, the absorption measurements at 870 nm are used because the BrC absorption is

negligible at this wavelength so any observed enhancement of absorption above the calculated BC absorption is from the lensing effect. The $E_{abs,mixing}$ values are used at all wavelengths because they are assumed independent of wavelength. The detailed information about the methods and calculations can be found in Zhang et al. [2016] and Cappa et al. [unpublished].

If $E_{abs,mixing}$ is set equal to 1, the BrC absorption would be equivalent to the difference between the observed absorption and the estimated absorption by uncoated BC, which means the contribution from lensing would be included as part of the BrC absorption. This approach is called the "upper-limit" approach in Cappa et al. [unpublished] as it gives the maximum of the possible BrC absorption. In contrast, if $E_{abs,mixing}$ is calculated as a function of R_{BC}, the resulting BrC absorption would only include the absorption of externally mixed BrC. This approach is called the "lensing-corrected" approach in Cappa et al. [unpublished] and gives the minimum of the possible BrC absorption. The lensing contribution can be evaluated as the difference between the two approaches. For the 2014 campaign, the lensing effect was measured to contribute 13% of absorption during daytime at 405 nm. In 2013, the lensing contribution is estimated based on core-shell Mie theory to be 14% on daily average because the measurements of enhancement are not available [*X L Zhang et al.*, 2016]. For both campaigns, the lensing effect contributes a rather small fraction (~10%) of the absorption at 405 nm. In this work, the reported BrC absorption from in situ measurements includes the contribution from lensing.

The measurements or estimates of lensing contributions is an important

difference between the in situ apportionment and the AERONET apportionment. As discussed before, most AAE methods including the Bahadur method assume the AAE values for the absorbing component to be intrinsic properties that are not dependent on the mixing state. However, the impact of internal mixing is included in their AAEs determined from spectral observations and correspondingly in the BC and BrC absorption calculated by their equations. These methodological differences could contribute to differences observed between the methods. However, for further comparisons, the in situ surface measurements need to be scaled to compare with AERONET measurements of the air column.

3.3 Scaling of surface measurements

To compare to the AERONET measurements of column measurements, estimates of column properties are made based on in situ surface measurements and the PBLH. PBL is the lowest part of the atmosphere with strong vertical mixing, which distributes aerosol mass from surface emissions throughout the layer [*Gobbi et al.*, 2004]. The top of the PBL is typically marked by a temperature inversion that traps the air within the PBL, separating it from the cleaner atmosphere above [*Cooper and Eichinger*, 1994; *Galchen et al.*, 1992]. The aerosol vertical distribution has frequently been found to be generally uniform within the PBL, indicating that the aerosols are well mixed by the strong turbulence in the PBL [*Li et al.*, 2017; *P F Liu et al.*, 2009; *Pringle et al.*, 2010; *Winker et al.*, 2013]. Two assumptions are made about the in situ surface-based estimates of column properties in this work: 1) the surface measurements of

extinction and absorption are representative of the AOD and AAOD in the PBL and 2) the AOD and AAOD values in the PBL account for most of the air column. The estimates of column properties based on surface measurements such as the absorption at 405 nm are calculated from:

$$AAOD405_{PBL} = b_{abs}405 \cdot PBLH \tag{7}$$

Analogous equations apply for the surface-based estimates of column extinction ($AOD405_{PBL}$) and the fraction of absorption due to BC ($AAOD405_{PBL,BC}$) and BrC ($AAOD405_{PBL,BrC}$).

For the 2013 campaign, the PBLH is obtained from the NOAA Air Resource Laboratory Real-time Environmental Applications and Display sYstem (Ready) using the North American Regional Reanalysis (NARR) dataset. PBLH simulations from NARR are available on a 3 hourly, 32 km grid from 1979 to the present. Since PBLH is affected by surface heat flux, which is mainly driven by solar radiation, the evolution of PBLH is directly related to the diurnal variation of temperature, and rapid changes are expected during morning and afternoon hours. The 3-hour time resolution may not capture the changing PBLH during these periods. Therefore, a smoothing spline function from Matlab is used to simulate 1 hour measurements based on the NARR dataset.

For the 2014 campaign, the PBLH is simulated from the Weather Research and Forecasting (WRF) Model. The WRF model uses inputs from the NARR model and produces simulations of PBLH with 1 hour resolution. The PBLH for both 2013 and 2014 campaign   has been converted to height above ground level.

The reliability of the simulated PBLH were accessed by comparing model performance for simulated surface temperature and wind speed, which are both related to PBLH. The WRF model performance has been checked in a 7-year simulation of the SJV compared to ARB surface observations. The mean fractional bias (MFB) of temperature and wind were generally within ± 15% [*Coniglio et al.*, 2010; *Hu et al.*, 2014; *Molders and Kramm*, 2010]. In addition, for the 2014 campaign, the PBLH simulated by the WRF model was generally within ± 180 m of simulations by the NARR model, and within ± 150 m of the simulations from Eta Data Assimilation System (EDAS) model. The NARR simulated results during the 2013 campaign were generally within ± 210 m of the EDAS simulations. The daytime hourly average throughout campaign (220 - 840 m from 9:00 AM to 3:00 PM) shows general agreement with the PBL observed (300 - 700 m) by flights circling Fresno and Bakersfield during DISCOVER-AQ [*Pusede et al.*, 2016]. Because the PBLH is applied to the surface measurements of both BC absorption and BrC absorption, the uncertainty in PBLH does not impact the fractions of BC and BrC determined from in situ measurements; however, it does impact the correlations between AERONET measurements and in situ surface-based column estimates.

3.4 Meteorology and other local conditions

Comparing the temperature, RH, visibility and PBLH between the 2013 and 2014 campaigns, the meteorological conditions are different, which could contribute to the comparisons between the AERONET measurements and the in situ

measurements (Figure.2). 115 level 1.5M AERONET measurements were collected during the 2013 campaign, which covered 4.2% of the time during the campaign, while 48 level 1.5M AERONET measurements were collected during the 2014 campaign, which covered 2.0% of the time (Table.2). There are two times more AERONET measurements in 2013 than in 2014 because more AOD measurements met the $AOD440_{COL} > 0.1$ threshold. This reflects the fact that the aerosol loadings were generally higher in 2013, which is consistent with the higher absorption measured at surface. The surface absorption at 405 nm ($b_{abs}405$) was on average 22.3 ± 9.7 Mm^{-1} during the 2013 campaign, which is substantially higher than the average of 14.7 ± 6.7 Mm^{-1} during the 2014 campaign. Young et al. [2016] suggested that the high surface absorption during the 2013 campaign was primarily driven by the enhanced emissions of residential wood burning for domestic heating due to the unusually cold temperatures (compared to a previous campaign at Fresno in 2010). This theory could help explain the observed difference in surface absorption between the 2013 and 2014 campaigns. The average temperature is similar for both campaigns (9.0 °C in 2013 and 9.1 °C in 2014), but the diurnal variation as the difference between daily maximum and minimum is 11.0 ± 3.8 °C in 2013, which is about 2 °C larger than that in 2014 (8.9 ± 3.1 °C). Therefore, the lower minimum temperature during the nighttime in 2013 is consistent with the higher peak of surface absorption related to residential burning.

The change of temperature also influences the change of PBLH. The most rapid change of temperature occurs from 9:00 AM to 11:00 AM, while the decrease in the afternoon is relatively slower. The most rapid change of PBLH occurs from 10:00 AM

to 12:00 PM for both campaigns, about 1 hour later than that of temperature. During

daytime (8:00 AM to 5:00 PM) the high PBLH (513 ± 294 m in 2013 and 463 ± 201 m

in 2014) indicates that the surface measurements were quickly diluted within the PBL.

High RH (> 80%) increases the particle light scattering due to water uptake by

a factor of 2 [*Kotchenruther et al.*, 1999; *Skupin et al.*, 2016]. However, the impact of

high RH on particle absorption is variable. Fresno typically has high RH during winter:

the campaign average RH is 72% in 2013 and 78% in 2014. However, the fact that

AERONET measures only during the daytime reduces the impact of humidity. The

average RH during the time of AERONET measurements is lower (60% in 2013 and

68% in 2014), suggesting that the influence from humidity might be small except during

the high-fog period (7 to 13 January 2015) of the 2014 campaign. The high-fog period

shows significantly lower visibility (3.0 ± 0.9) than the campaign average in 2014 (9.1

± 1.4 km) and 2013 (10.5 ± 1.7 km). The surface absorption during the high-fog period

is higher (18.9 ± 4.4 Mm^{-1}) than the campaign average in 2014 (14.7 ± 6.7 Mm^{-1}), but

still lower than that during the 2013 campaign (22.3 ± 9.7 Mm^{-1}). The high (> 80%) RH

that persisted till 11:00 AM during the high-fog period indicates that the morning

measurements could have been affected by the difference between the ambient

conditions in which AERONET measurements were made and the dry conditions (RH

< 30%) in which in situ measurements were collected.

Surface XRF analysis and AERONET parameters indicate that the dust

contribution to absorption is low during both campaigns. Specifically, the 20 PM1 and

5 PM2.5 filter samples from the 2014 campaign show that dust contributes only 3% of

PM1 and 5% of PM 2.5 based on XRF analysis (Chester Laboratories). For the AERONET measurements, the average SAE1 is 1.56 ± 0.31 and the average AAE2/AAE1 is 1.03 during the 2014 campaign, indicating that most of the measurements fit the dust-free conditions of the Bahadur method (i.e. SAE1 > 1.2 or AAE2/AAE1 > 0.8). The conditions are evaluated from the average properties during the campaign rather than each individual measurement here because the level 1.5M measurements have larger uncertainty compared to the level 2.0 measurements used by Bahadur et al. [2012]. For the 2013 campaign, the average SAE1 is 1.58 ± 0.30 and average AAE2/AAE1 is 1.04, which also fits the dust-free conditions. Therefore, the 2013 campaign is also assumed to have low dust influence based on AERONET parameters although filter measurements of dust are not available for the campaign.

The low dust conditions at Fresno leads to a large fraction of negative results (43% in 2013 and 51% in 2014) in the apportionment. While some small negative values of BC, BrC or dust might be due to noise, large negative values suggest that the conditions contradict the assumptions of the Bahadur method, and the equation needs to be modified. Based on the assumption that the 2013 and 2014 campaigns have low dust influence, equation 4 is modified to be:

$$AAOD(\lambda_i)=AAOD_{ref,BC}\left(\frac{\lambda_i}{\lambda_{ref}}\right)^{-AAE_{BC,i}}+AAOD_{ref,BrC}\left(\frac{\lambda_i}{\lambda_{ref}}\right)^{-AAE_{BrC,i}} \tag{8}$$

With fewer unknowns, only AAOD at 440 nm and 675 nm and AAE1 between these two wavelengths are needed to calculate the fractions of AAOD from the two absorbing components at wavelength (λ_i).

Section 4 Discussion

4.1 Comparison of results in this work with other studies

During the 2013 campaign, the AERONET apportionment shows that BC contributes 67% and BrC contributes 33% of the absorption at 440 nm. The in situ apportionment shows that BC contributes 89% and BrC contributes 11% of absorption at 405 nm. During the 2014 campaign, the fraction is 72% BC and 28% BrC from AERONET. The fraction is 68% BC and 32% BrC from the in situ apportionment.

The AERONET apportionment of BC and BrC from both campaigns fall in the general range given by values reported in previous AERONET observationally constrained studies (Table.3). Using concepts similar to those of the AERONET-AAE methods, studies found BrC contributes on average 0 - 40% of the global absorption at 440 nm, and on average 28% at 10 AERONET sites around California [*Bahadur et al.*, 2012; *X Wang et al.*, 2016b]. The AERONET apportioned BrC from both 2013 and 2014 (28-33%) is consistent with this reported range. The BrC absorption is 39 - 49% of BC absorption for both campaigns, which is at the mid-range of 27 - 70% of BC absorption predicted by the global Integrated Massively Parallel Atmospheric Chemical Transport (IMPACT) model [*Lin et al.*, 2014].

The in situ apportionment of BC and BrC in 2014 is in the general range (50 - 85% for BC, 15 - 50% for BrC at wavelengths shorter than 500 nm) given by previous surface absorption studies that focused on areas with similar biomass burning aerosols or biomass burning influenced aerosols. On the other hand, the fractions in

2013 are at the high end of BC and low end of BrC of the general range. For locations with significant residential burning, like Fresno, BrC absorption during daytime is lower than during nighttime [*X L Zhang et al.*, 2016]. Therefore, the low BrC fraction and complementary high BC fraction in 2013 could be explained by the selection of daytime measurements (in order to compare with AERONET measurements that are only made during daytime) and by the stronger diurnal variation in 2013 compared to 2014.

In Section 4.2, the agreement between AERONET apportionment and in situ apportionment was evaluated by comparisons of AERONET AOD, AAOD as well as its apportionment to BC and BrC with in situ surface-based column estimates of corresponding properties in the PBL.

4.2 Comparison of AOD and AAOD

The AOD comparison and the AAOD comparison show stronger correlations with time for the 2014 campaign than for the 2013 campaign (Figure.3). During the two campaigns, there are 163 AERONET measurements that fit the level 1.5M criteria (listed in Table.2) of daytime, clear sky, and high AOD (AOD440 > 0.1). Of these 163 measurements, 146 measurements correspond in time with in situ measurements. These 146 AERONET measurements cover 4.2% of the time during the 2013 campaign and 2.0% of the time during the 2014 campaign. In this work, the square of the correlation coefficient (R^2) from linear regression by least-squares with $R^2 \geq 0.64$ are considered strong; correlations with $0.64 > R^2 > 0.25$ are considered moderate;

34

correlations with $0.25 \geq R^2$ are considered weak [*Devore and Berk*]During the 2014 campaign, the AERONET $AOD440_{COL}$ correlates strongly ($R^2 = 0.82$) to the in situ $AOD405PBL$ and the AERONET $AAOD440COL$ correlates moderately ($R^2 = 0.60$) to the in situ $AAOD405PBL$ (Table.4; Figure.3b,3d). For these correlations, the fitted slope of AERONET $AOD440_{COL}$ to in situ $AOD405_{PBL}$ is 1.06, and the fitted slope of AERONET $AAOD440_{COL}$ to in situ $AAOD405_{PBL}$ is 1.23, respectively. The slopes near 1 indicates good agreement between the AERONET measurements and in situ estimates. Since in situ AOD and AAOD estimates do not include the air column above the PBL, the higher than unity slopes are consistent with expectations. The positive intercepts, on the other hand, suggest that the AERONET measurements could be biased high at low AOD and AAOD values.

In contrast, the slopes are less than unity and the correlations are below $R^2 = 0.5$ during the 2013 campaign (Figure.3a,3c). The correlation between AERONET $AOD440_{COL}$ and in situ $AOD405_{PBL}$ is $R^2 = 0.42$ and the correlation between AERONET $AAOD440_{COL}$ and in situ $AAOD405_{PBL}$ is $R^2 = 0.32$. The fitted slope of AERONET $AOD440_{COL}$ to in situ $AOD405_{PBL}$ is 0.42 and the fitted slope of AERONET $AAOD440_{COL}$ to in situ $AAOD405_{PBL}$ is 0.79. The low correlations and the slopes far from 1 indicate less agreement between the AERONET measurements and the in situ estimates during the 2013 campaign. The lower than unity slopes suggest that for some individual measurements in 2013, scaling the surface measurement to the modeled PBL over-estimates both AOD and AAOD with respect to the AERONET measurements. The reason for this over-estimation could be either that the surface

measurements are higher than the averages in the PBL or that the PBLHs simulated from NARR model are different from the actual values. To distinguish between these two causes, the correlation between the AERONET measurements and the in situ surface measurements is analyzed for both campaigns (Table.4). Most of the AERONET measurements during the 2013 campaign (61%) and the 2014 campaign (63%) were made from 12:00 PM to 4:00 PM when the average PBLH is 765 ± 384 m in 2013 and 617 ± 251 m in 2014, and the average difference between maximum and minimum height during this period is 330 ± 230 m in 2013 and 310 ± 113 m in 2014. Since the PBLHs are relatively constant, the column properties are more likely to be related to the surface measurements than they would be when PBLH are changing rapidly. It turns out that the observations are consistent with this expectation in 2014, but not in 2013. The $AOD440_{COL}$ correlates with $b_{ext}405$ moderately ($R^2 = 0.56$) in 2014, but weakly ($R^2 = 0.07$) in 2013. Similarly, the $AAOD440_{COL}$ correlates with $b_{abs}405$ moderately ($R^2 = 0.31$) in 2014, but weakly ($R^2 = 0.03$) in 2013. The better correlations of 2014 surface measurements with the AERONET measurements indicates that they better represent the column properties in the PBL than in 2013.

The correlations between the AERONET AAOD measurements and in situ AAOD estimates are lower than that between the AOD measurements and estimates (the difference in R^2 is -0.12 in 2013 and -0.22 in 2014) . The lower correlations of AAOD compared to AOD is likely from the higher uncertainty contributed by the AERONET SSA retrievals that are used in AAOD calculations. The fitted slopes of AERONET AAOD measurements to in situ AAOD estimates are higher than that of

AOD measurements to estimates (the slope increases from 0.42 to 0.79 in 2013, and from 1.06 to 1.23 for 2014). The AERONET retrieved SSAs (0.93 ± 0.02 during both campaigns) are similar to the in situ measured SSAs (0.94 ± 0.02 in 2013, 0.95 ± 0.02 in 2013), even though the in situ measurements were made in dry condition (RH<30) while the AERONET measurements were made in ambient environment with higher RH (average 57% in 2013, and 61% in 2014). The enhancement in the particle extinction and absorption due to high RH will be discussed in the section of uncertainties.

4.3 Comparison of BC and BrC fractions

The BC comparisons show better correlations with respect to time than that of the BrC comparisons (Figure.4). The AERONET apportionment of column absorption to BC and BrC are based on the AAOD measurements, therefore the same criteria (level 1.5M) and limitations are applied.

During the 2014 campaign, the AERONET $AAOD440_{COL,BC}$ correlates moderately with the in situ $AAOD405_{PBL,BC}$ (R^2 = 0.49) (Figure.4b). The fitted slope of AERONET $AAOD440_{COL,BC}$ to in situ $AAOD405_{PBL,BC}$ is 1.18. The moderate correlation and the close to unity slope indicate general agreement between AERONET $AAOD440_{COL,BC}$ and in situ estimated $AAOD405_{PBL,BC}$. The consistently higher BC absorption apportioned from the AERONET measurements than the in situ estimated values in PBL is consistent with expectations. The AERONET $AAOD440_{COL,BrC}$ turns out to correlate moderately with the in situ $AAOD405_{PBL,BrC}$ (R^2 = 0.29) (Figure.4d).

37

However, higher correlations ($R^2 > 0.5$) are found between AERONET AAOD440$_{COL,BrC}$ and in situ surface measurements of $b_{ext}405$ as well as AERONET AOD440$_{COL}$ (Table.4). The higher correlations with both in situ surface ambient measurements and AERONET ambient measurements suggest the apportioned AAOD to BrC is subject to background noise. There is also a moderate correlation ($R^2 = 0.33$) between AERONET AAOD440$_{COL,BrC}$ and PBLH simulated by the WRF model, which suggests the correlation between AERONET apportionment and in situ estimates could be caused by the scaling factor. In addition, the lower than unity slope (0.62) of AERONET AAOD440$_{COL,BrC}$ to in situ AAOD405$_{PBL,BrC}$ suggests that the in situ measurements over-estimate column properties compared to AERONET at high AAOD.

For the 2013 campaign, the correlation between AERONET AAOD440$_{COL,BC}$ and in situ AAOD405$_{PBL,BC}$ is $R^2 = 0.28$ and the correlation between AERONET AAOD440$_{COL,BrC}$ and in situ AAOD405$_{PBL,BrC}$ is $R^2 = 0.15$. The low correlations are consistent with expectations since the correlation between AERONET measurements and in situ estimates of AAOD is already low ($R^2 = 0.30$). The additional uncertainties contributed by the apportionment methods means the correlations of apportioned components from AAOD would not exceed the correlation of AAOD itself. The fitted slope of AERONET AAOD440$_{COL,BC}$ to in situ AAOD405$_{PBL,BC}$ is 0.61 and the fitted slope of AERONET AAOD440$_{COL,BrC}$ to in situ AAOD405$_{PBL,BrC}$ is 0.67. The lower than unity slopes are consistent with the results of the AOD and the AAOD comparisons.

During both campaigns, the correlations between the AERONET AAOD440$_{COL,BC}$ and in situ AAOD405$_{PBL,BC}$ have correlations closer to that between

AERONET AAOD440$_{COL}$ and in situ AAOD405$_{PBL}$, especially in 2014. In addition, the fitted slope of AERONET AAOD440$_{COL,BC}$ to in situ AAOD405$_{PBL,BC}$ in 2014 shows close agreement to that of AERONET AAOD440$_{COL}$ to in situ AAOD405$_{PBL}$ (the slopes are 1.18 for BC, 0.62 for BrC, and 1.23 for AAOD). The similar slopes suggest the agreement between apportioned BC is better than that of BrC because BC is the major contributor of absorption.

4.4 Fractions and uncertainties

BC is identified as the larger absorber during both the 2013 and 2014 campaigns; both the AERONET apportionment and in situ apportionment show that BC absorbs generally two times higher than BrC (Figure.5). The BC fraction from the AERONET apportionment is 4% higher than that from the in situ apportionment in 2014; in 2013, the BC fraction from the AERONET apportionment is 22% lower than that from the in situ apportionment. The smaller difference in BC fraction between AERONET and in situ apportionment is consistent with the better correlation between AERONET AAOD440$_{COL,BC}$ and in situ AAOD405$_{PBL,BC}$ during the 2014 campaign.

Since BrC has AAE higher than 1, the contribution of BrC at 405 nm is higher than at 440 nm. If the AAE of BrC between 405 and 675 nm is the same as the AAE between 440 and 675 nm, the corresponding BrC absorption at 405 nm can be calculated as:

$$AAOD405_{COL,BrC}=AAOD675_{COL,BrC}\left(\frac{405}{675}\right)^{-AAE1_{BrC}}=AAOD440_{COL,BrC}*1.46 \qquad (9)$$

This shows that the BrC absorption at 405 nm would be 46% higher than at 440

nm. For BC, the AAE is less than that of BrC and the increase would be 5% from 440 nm to 405 nm. However, because BC contributes at least 67% of absorption at 440 nm, the resulting change in fraction is at most 7%. Therefore, although the AERONET measurements and in situ measurements were made at different wavelengths, the impact on BC and BrC fractions is small compared to the uncertainty.

The measurement uncertainty of AERONET AAOD depends on the corresponding AOD and SSA values; at low AOD ($AOD440_{COL}$ < 0.2), the measurement uncertainty is ± 0.01 for AOD and ± 0.03 - 0.07 for SSA [*Dubovik et al.*, 2002]. Measurements of $AAOD440_{COL}$ below 0.01 have uncertainties higher than 100% and are considered to be below the detection limit. The average of level 1.5M $AAOD440_{COL}$ is 0.011 ± 0.0039 in 2013 and 54% of measurements are above the detection limit. The average is 0.011 ± 0.0044 in 2014 and 56% of measurements are above the detection limit. The average uncertainty of AERONET AAOD measurements above 0.01 is 74%. If $AAOD440_{COL}$ measurements below the detection limit are replaced by the mid-range value of 0.005, the average AAOD would be 0.010 ± 0.0049 in 2013, and 0.010 ± 0.0052 in 2014. The small difference (~10%) between average AAOD with and without replacement of measurements below the detection limit suggests that the uncertainty of AAOD would have a rather small impact on the fractions of BC and BrC. However, the uncertainty of the AAE values used in apportionment could be substantial since the AERONET-AAE method depends on AAE exponentially. The sensitivity of AERONET apportionment to the AAE values is examined by considering alternate values for AAE of BC and BrC (Table.5). The

sensitivity test shows that the change of BC absorption from AERONET apportionment could be up to 29% with the range for AAE of BC of 0.55 ± 0.24 and BrC of 4.55 ± 2.01 given by Bahadur et al. [2012] and up to 44% with the wider range of AAE from other studies (Table.1).

In addition, the discrepancy between the AERONET apportionment and the in situ apportionment could be caused by absorption in the layers above the PBL that are included in AERONET but not surface measurements. The in situ $AAOD405_{PBL}$ estimates are on average 69% of the AERONET $AAOD440_{COL}$ in 2013 and 57% in 2014, indicating the contribution from other layers might be significant. Liu et al. [2014] found that both BC and BrC are present throughout the tropospheric column (<13 km) and the fraction of BrC relative to BC increased with altitude due to contributions from secondary sources. This could be the reason why the BrC fraction from in situ surface measurements is 22% lower than that from AERONET measurements in 2013. Studies also observed long-range transport dust from Asia and the Sahara present in cloud layers over California, especially in winter and spring [*Fan et al.*, 2014; *Pratt et al.*, 2009]. Therefore, aerosols in the layers above the PBL could contribute to the column properties with chemical compositions different from the near surface layer.

Section 5 Conclusion

This work analyzes the BC and BrC absorption determined from AERONET and in situ observations during winter campaigns in 2013 and 2014 at Fresno, CA. The fractions of BC and BrC at 440 nm are apportioned from AERONET AAOD with level 1.5M criteria using the AERONET-AAE method modified for the measured local low-dust conditions. The fractions from in situ measurements are apportioned using a combination of the MAC and TD methods. The in situ measurements are expected to give a more precise determination of BC and BrC absorption because they do not rely on global average AAE values, but they only measured at the surface. The AERONET measures column properties using AAE values that are assumed to be globally representative of BC and BrC independent of location and mixing state. Therefore, the comparison between BC and BrC absorption from AERONET and in situ apportionment illustrates the extent to which the surface measurements could be used to estimate column properties and to which the AERONET measurements are representative of surface absorption.

The fractions of BC and BrC from AERONET in both campaigns are consistent with the range reported in previous studies using AERONET spectral measurements and model simulations. The fractions calculated from AERONET apportionment (72% BC and 28% BrC) in 2014 are close to the fractions calculated from in situ apportionment (68% BC, 32% BrC including contribution from internal mixing). The in situ estimates of AAOD in the PBL by scaling surface measurements to modeled PBLH show good correlation ($R^2 = 0.60$) with AERONET AAOD in 2014. Similarly, the in situ

42

estimates of BC absorption in the PBL show a good correlation (R^2 = 0.49) of the AERONET AAOD apportioned to BC. The good correlations indicate that when the assumptions that the surface measurements are representative of properties in the PBL and that the PBL accounts for most of the air column are met, the AERONET-AAE method modified based on local measurements gives apportionment of BC and BrC absorption that agrees with the in situ apportionment. In contrast, the AERONET apportionment of 67% BC and 33% BrC in 2013 is different from the 89% BC and 11% BrC (including the contribution from internal mixing) from in situ apportionment. The weaker correlation of AERONET AOD to in situ surface measurements of extinction coefficients in 2013 (R^2 = 0.07) than that in 2014 (R^2 = 0.56) indicates that the surface measurements in 2014 are more representative of the column properties than in 2013. This difference in correlation indicates that when the surface measurements are not representative of properties in the PBL or the PBL does not account for most of the air column, then scaling surface measurements to the modeled PBLH does not provide good estimates of column properties.

The extent of the agreement between AERONET apportionment using the AERONET-AAE method and in situ apportionment might be limited by the fact that relatively small contributions from lensing (~10%) were estimated from the surface measurements during both campaigns. A larger impact of lensing of up to a factor of two has been estimated by models and measured in lab experiments [*Cappa et al.*, 2012; *S H Chung and Seinfeld*, 2005; *Jacobson*, 2001; *Schnaiter et al.*, 2005; *Slowik et al.*, 2007]. The observations from field campaigns focused on urban areas, however,

have found enhancement measurements with variability that both agree and contradict the theoretical calculation and laboratory measurements [*Cappa et al.*, 2012; *Healy et al.*, 2015; *Knox et al.*, 2009; *D Liu et al.*, 2017; *S Liu et al.*, 2015b].

This work shows that additional research using both AERONET and in situ approaches is needed to assess the extent to which AERONET apportionment could be used to provide estimates of BC and BrC absorption across the nearly global AERONET network. The large measurement uncertainty and bias toward high aerosol loadings in the current AERONET products might be improved with retrieval algorithms that are more sensitive to aerosol absorption measurements. The AERONET-AAE method could be less dependent on the AAEs of BC and BrC by explicitly including the contribution from lensing. In terms of the in situ approaches, the usage of the surface measurements to estimate column properties could be improved by a better understanding of the aerosol chemical composition in the vertical distribution, which could give more direct comparison to the AERONET apportionment.

This thesis, in part is currently being prepared for submission for publication of the material. Chen, Sijie; Cappa, Christopher; Ramanathan, Veerabhadran; Russell, Lynn; Zhang, Xiaolu. The thesis author was the primary author of this material.

Section 6 Figures and tables
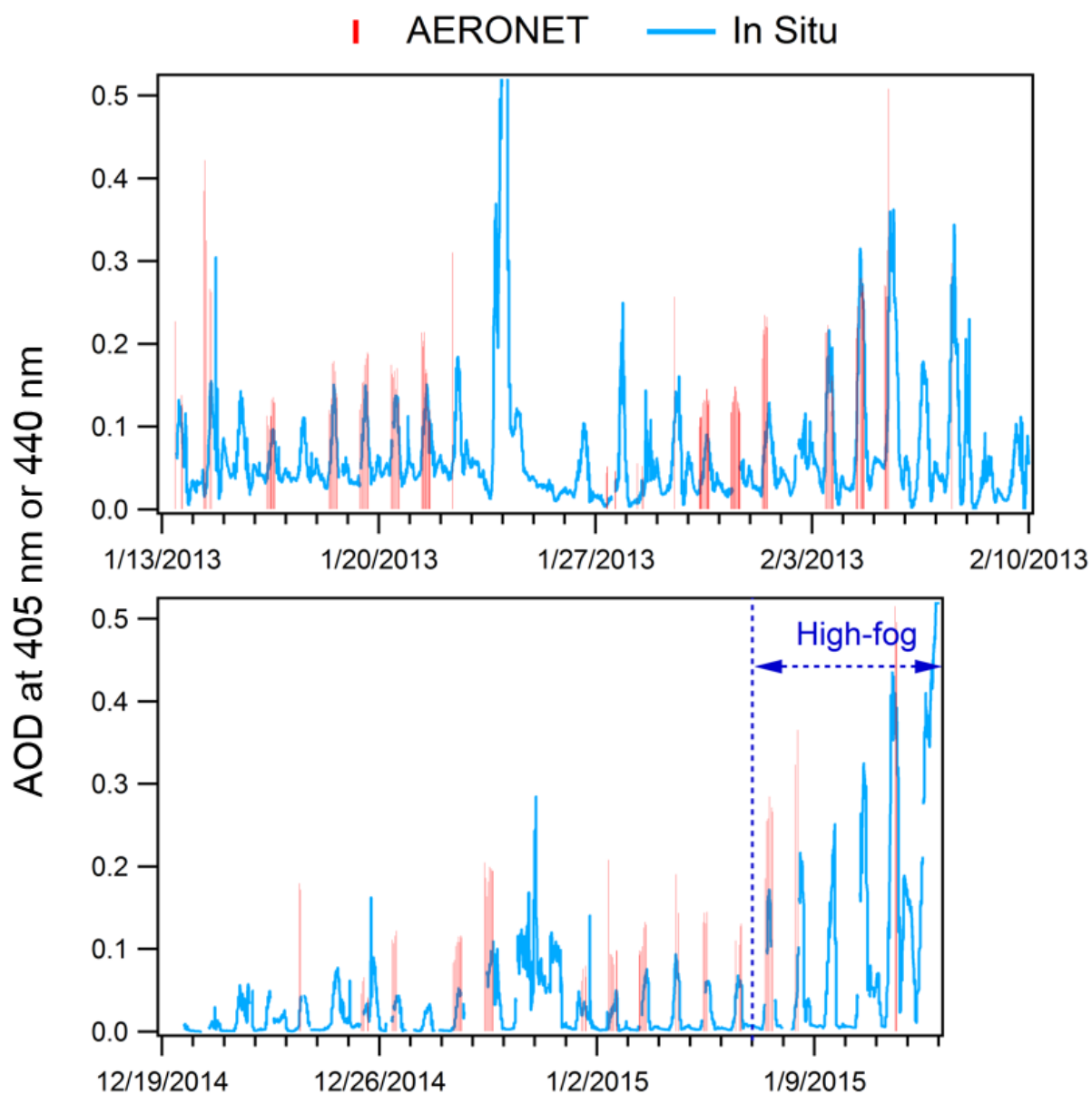
Figure 1 Time series of AERONET AOD measurements at 440 nm and in situ surface-based estimates of extinction within the PBLH at 405 nm (babs405 x PBLH) during the 2013 (above) and 2014 (below) campaigns. The period from 7 to 13 January 2015 is labeled as the high-fog days for high RH (persistently at or above 90% from 22:00 to 9:00) and low visibility (1.6 - 3.2 km from 22:00 to 9:00).
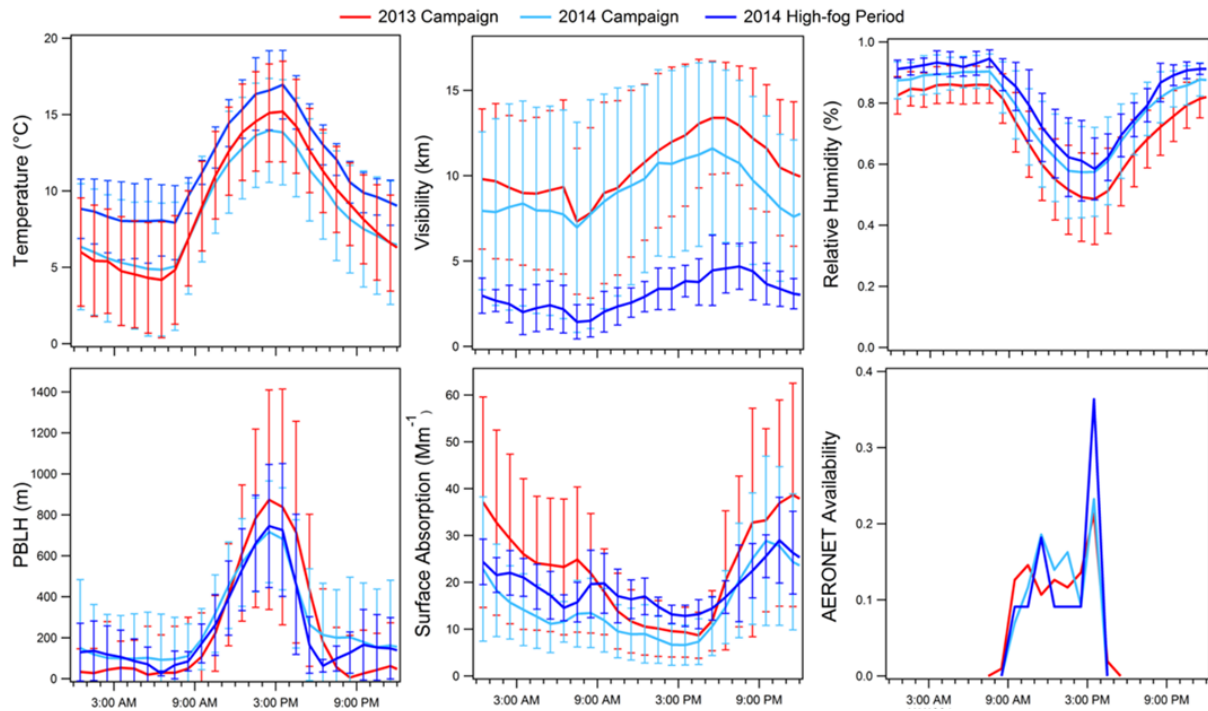
Figure 2 Hourly average of meteorological conditions (temperature, relative humidity, visibility and PBLH), surface absorption (babs405) and AERONET measurements availability observed during the 2013 and 2014 campaigns. AERONET measurements availability is defined as fraction of the total account of measurements. Error bars show the standard deviation of the hourly average.
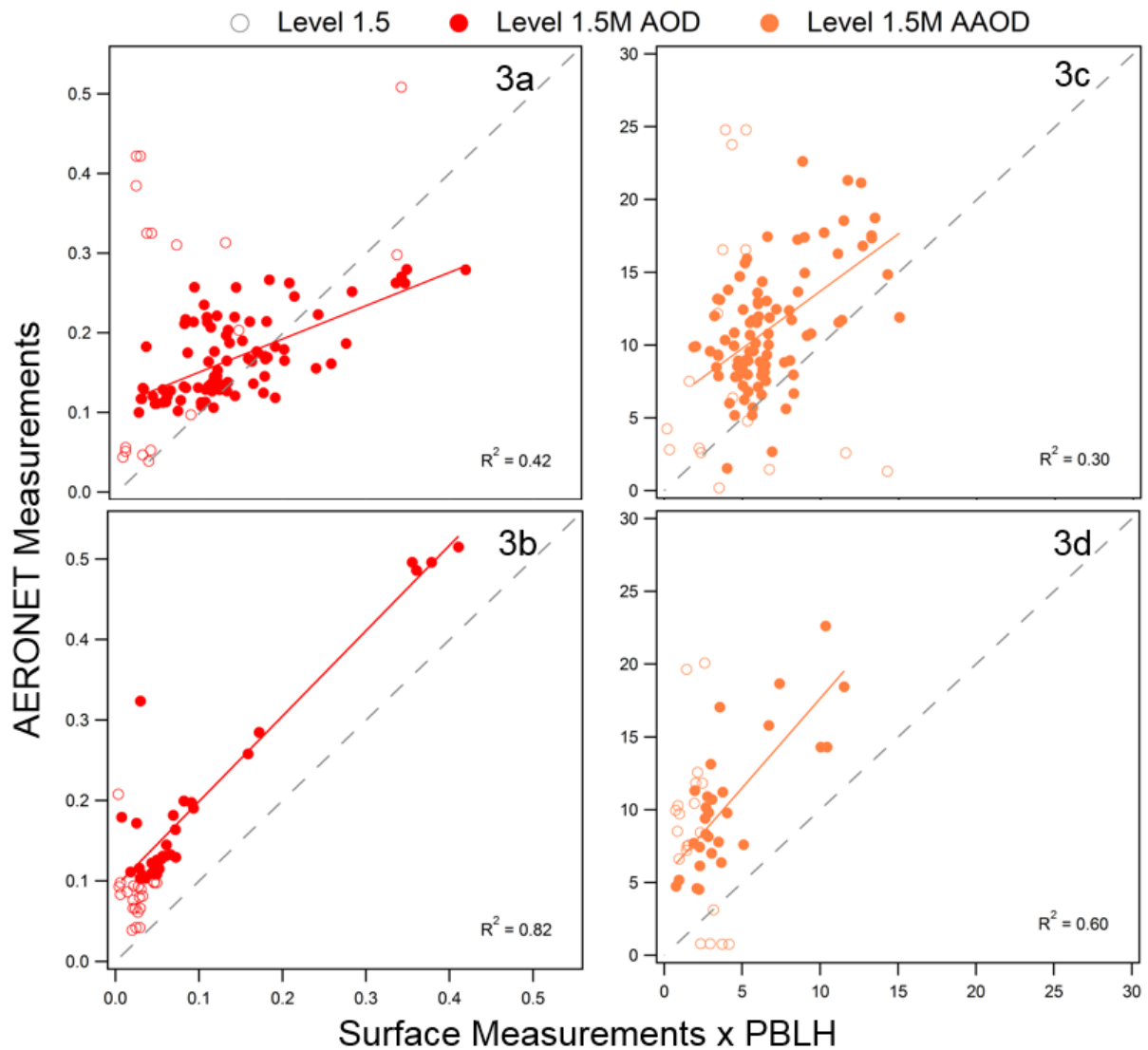
Figure 3 AOD and AAOD comparisons from the 2013 campaign (above) and the 2014 campaign (below). Empty circles show level 1.5 AERONET measurements that correlate with the in situ measurements; solid circles (red for AOD, orange for AAOD) show level 1.5M AERONET measurements that fit quality criteria: 1) AOD440 > 0.1; 2) SSA440 within 95% confidence intervals for the mean of a log-normal distribution and correlate with the in situ measurements. Left plots (3a,3b) compare AERONET $AOD440_{COL}$ with in situ $AOD405_{PBL}$ ($b_{ext}405$ x PBLH); right plots (3c,3d) compare AERONET $AAOD440_{COL}$ with in situ $AAOD_{PBL}$ ($b_{abs}405$ x PBLH). PBLH is simulated from NARR model for 2013 and from WRF model for 2014. Gray line is 1-to-1 ratio line. Regression lines give the slope and the correlation coefficient R^2.
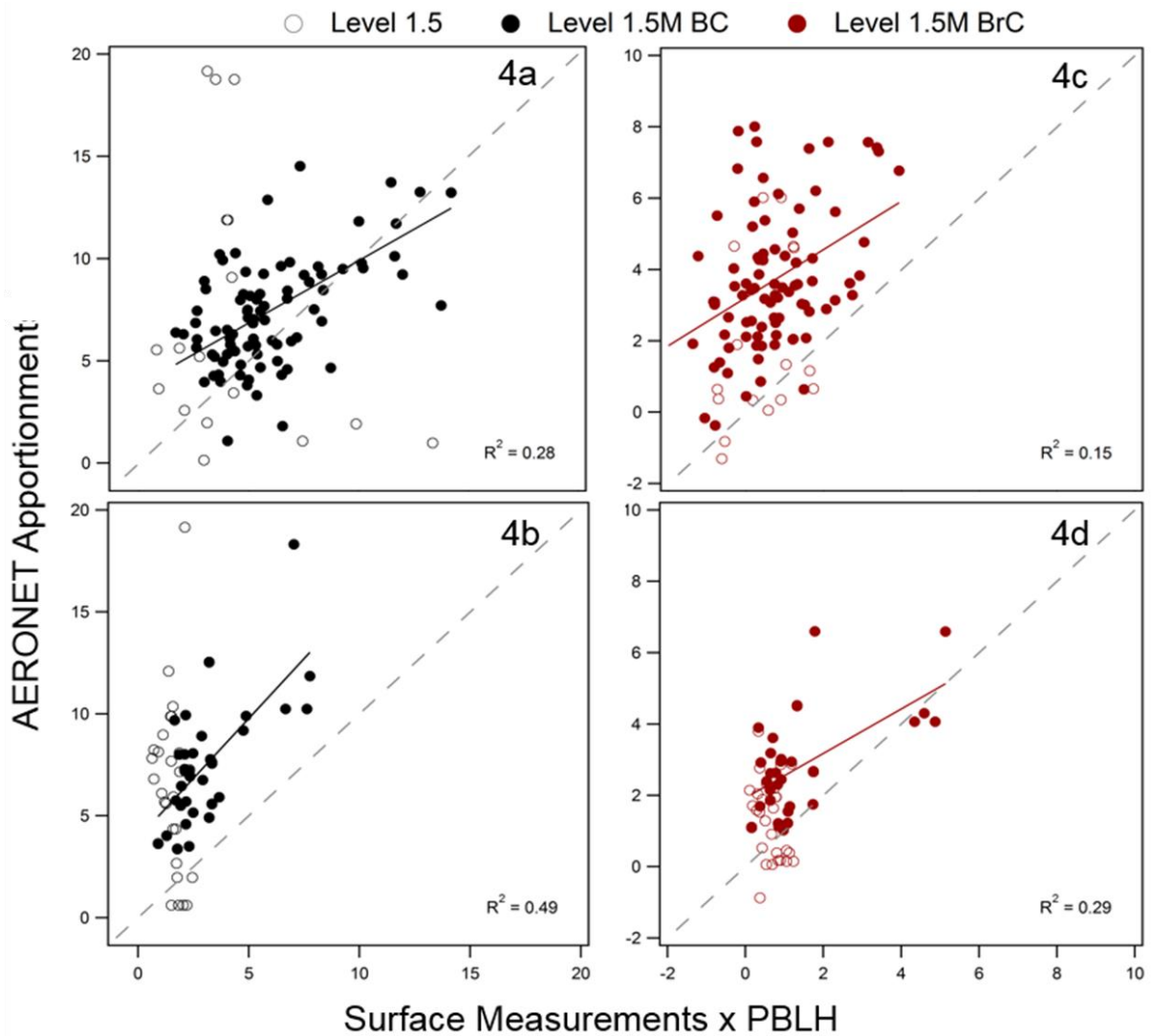
Figure 4 BC and BrC comparisons from the 2013 campaign (above) and the 2014 campaign (below). Empty circles show the apportionment from level 1.5 AERONET AAOD that correlate with the in situ measurements; solid circles (black for BC, brown for BrC) show the apportionment from level 1.5M AERONET AAOD that fit quality criteria: 1) AOD440 > 0.1; 2) SSA440 within 95% confidence intervals for the mean of a log-normal distribution and correlate with the in situ measurements. Left plots (4a,4b) compare AERONET AAOD440$_{COL,BC}$ with in situ AAOD405$_{PBL,BC}$ ($b_{abs,BC}$405 x PBLH); right plots (4c,4d) compare AERONET AAOD440$_{COL,BrC}$ with in situ AAOD405$_{PBL,BrC}$ ($b_{abs,BrC}$405 x PBLH). PBLH is simulated from NARR model for 2013 and from WRF model for 2014. Gray line is 1-to-1 ratio line. Regression lines give the slope and the correlation coefficient R^2.
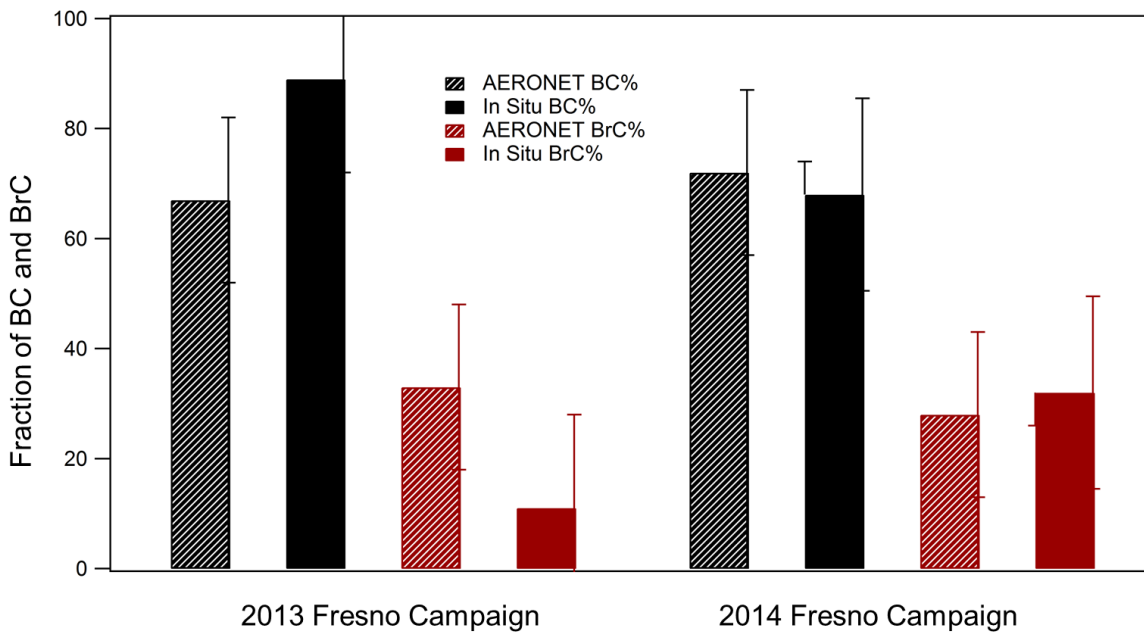
Figure 5 Fractions of BC and BrC from the AERONET apportionment of AAOD at 440 nm and from the in situ apportionment of surface absorptions at 405 nm. The Error bars on right edge indicates uncertainties. The uncertainty of AERONET fractions is from the sensitivity to the AAE values used in apportionment. The uncertainty of in situ method is from the measurement uncertainties from instruments and propagate through calculations. The error bar on right edge for in situ measurements in 2014 indicate the BC fraction could be high and BrC fraction could be lower if not count coating contribution as part of BrC absorption. This is also true for 2013 but can't be quantified due to lack of observation in 2013.

Table 1 Literature review of comparable AAE values to BC and BrC from previous studies.

Citation	Comparable to BC		Comparable to BrC	
	Measured Constituents	AAE (λ in nm)	Measured Constituents	AAE (λ in nm)
Cappa et al., [unpublished]	BC Fresno 2014	0.89 (405 – 532)	BBOA Fresno 2014	2.37 (405 – 532)
[Fuller et al., 2013]	BC London	0.96 (370 – 880)		
[Lack and Langridge., 2013]	BC Varied	0.8 - 1.4 (467 – 660)		
[Bahadur et al., 2012]	BC/soot/EC AERONET Sites	0.55 ± 0.24 (440 – 675)	OC AERONET Sites	4.55 ± 2.01 (440 – 675)
[Lack et al., 2012]	BC Boulder	1.1 - 1.4 (404 – 658)	POM Boulder	1.25 - 2.3 (404 – 658)
[Gyawali et al., 2011]	BC Reno, USA	1.0 - 1.1 (405 – 870)		
[Sandradewi et al., 2008]			OC Switzerland	1.8 - 1.9 (470 – 950)
[Schnaiter et al., 2006]			OC Chamber	2.2 - 3.5 (450 – 550)
[Hoffer et al., 2005]	Diesel Soot LBA-SMOCC	1.056 (300 – 700)	HULIS LBA-SMOCC	6 - 7 (300 – 700)
[Kirchstetter et al., 2004]	BC SAFARI, LBNL	0.6 - 1.3 Varied	OC Urban Vehicle	4.69 (350 – 550)
[Schnaiter et al., 2003]	Diesel Soot AIDA	1.1 (450 – 700)		

50

Table 2 AERONET quality assurance criteria at each level and corresponding data availability during 2013 and 2014 Fresno campaigns

	Major Criteria*	2013 Campaign Measurements (Time%)	2014 Campaign Measurements (Time%)
Level 1.5	Automatic cloud-screening	125 (4.7%)	69 (2.9%)
Level 1.5M	Automatic cloud-screening AOD440 > 0.1 SSA440 within 95% confidence intervals for the mean of a log-normal distribution	115 (4.2%)	48 (2.0%)
Level 2.0	Criteria for level 1.5 AOD440 > 0.4	0 (0%)	2 (0.08%)

*: The complete quality assurance criteria for level 1.5 and level 2.0 could be found in Holben et al. [2006]

Table 3 Literature review of BC and BrC absorption contribution from previous studies.

	Citation	BC Absorption (λ nm)	BrC Absorption (λ nm)	Notes
Column (AERONET) Measurements	This work Fresno 2014	72% (440)	28% (440)	
	This work Fresno 2013	67% (440)	33% (440)	
	[Wang et al., 2016] Global AERONET sites		0 - 40% (440)	
	[Bahadur et al., 2012] California AERONET sites	58% (440)	28% (440)	Additional 16% contribution from dust
Surface Measurements	This work Fresno 2014	68% (405)	19% (405)	Additional 13% contribution from lensing
	This work Fresno 2013	89% (405)	11% (405)	BrC absorption includes contribution from lensing
	[Lack et al., 2012] Four-Mile Canyon fire 2010	54% ± 16% (404)	27 ± 15% (404)	Additional 19 ± 8% from lensing
	[Yang et al., 2009] EAST-AIRE	85% ± 19~26% (470)	15% (470)	
	[Hoffer et al., 2006] LBA-SMOCC 2002	50% - 65% (300)	35% - 50% (300)	

Table 4 Correlation coefficients for linear relationships between in situ surface measurements, PBLH, in situ column estimates and AERONET measurements. The values in the table are calculated using in situ measurement corresponding to 15 minutes interval with AERONET measurement. The values in in parentheses are calculated using all day time measurement, which refers to the period from 1 hour after sunrise to 1 hour before sunset.

2013 Fresno		AERONET Measurements and Apportionment				Model Results
Correlation Coefficient R^2		AOD 440_{COL}	AAOD 440_{COL}	AAOD $440_{COL,BC}$	AAOD $440_{COL,BrC}$	PBLH
Model Results	PBLH	0.08	0.02	0.05	0.00	--
Surface Measurements	$b_{ext}405$	**0.07**	0.00	0.05	0.09	-0.13 (-0.23)
	$b_{abs}405$	0.03	**0.03**	0.00	0.07	-0.46 (-0.38)
	$b_{abs}405_{BC}$	0.04	0.00	**0.03**	0.07	-0.36 (-0.42)
	$b_{abs}405_{BrC}$	0.01	0.00	-0.01	**0.04**	-0.29 (-0.15)
Column Estimates	AOD405$_{PBL}$	**0.42**	0.26	0.20	0.15	0.31 (0.17)
	AAOD405$_{PBL}$	0.18	**0.30**	0.17	0.26	0.26 (0.12)
	AAOD405$_{PBL,BC}$	0.20	0.32	**0.28**	0.14	0.36 (0.25)
	AAOD405$_{PBL,BrC}$	0.01	0.00	0.01	**0.15**	**0.08 (-0.06)**
2014 Fresno		AERONET Measurements and Apportionment				Model Results
Correlation Coefficient R^2		AOD 440_{COL}	AAOD 440_{COL}	AAOD $440_{COL,BC}$	AAOD $440_{COL,BrC}$	PBLH
Model Results	PBLH	0.21	0.10	0.13	0.03	--
Surface Measurements	$b_{ext}405$	**0.56**	0.52	0.34	0.67	-0.00 (-0.01)
	$b_{abs}405$	0.16	**0.31**	0.17	0.50	-0.18 (-0.12)
	$b_{abs}405_{BC}$	0.12	0.23	**0.11**	0.42	-0.25 (-0.20)
	$b_{abs}405_{BrC}$	0.64	0.54	0.40	**0.59**	0.02 (-0.01)
Column Estimates	AOD405$_{PBL}$	**0.82**	0.38	0.40	0.22	0.18 (0.21)
	AAOD405$_{PBL}$	0.64	**0.60**	0.42	0.25	0.23 (0.27)
	AAOD405$_{PBL,BC}$	0.64	0.39	**0.49**	0.25	0.28 (0.32)
	AAOD405$_{PBL,BrC}$	0.70	0.35	0.42	**0.29**	**0.33 (0.36)**

Table 5 Uncertainty (% Change) in the AAOD apportioned BC resulted from changes on the AAE values.

	AAE BC (440-675 nm)	AAE BrC (440-675 nm)	BC% at 440 nm	BC% Change
Reference AAE	0.55	4.55	72%	0
Sensitivity Test of BC Values	**0.67**	4.55	76%	6%
	0.79	4.55	81%	13%
Sensitivity Test of BrC Values	0.55	**2.55**	51%	-29%
	0.55	**3.55**	60%	-17%
	0.55	**5.55**	80%	11%
	0.55	**6.55**	87%	21%
Sensitivity Test of Both Values	**0.89**	**2.37**	102%	42%
	1.0	**4.4**	91%	26%
	1.4	**7**	104%	44%

*: Change in BC% change is defined as percentage change in the apportioned BC fraction relative to that derived from the reference AAE used in this work.

References

Andreae, M. O. & A. Gelencser (2006) Black carbon or brown carbon? The nature of light-absorbing carbonaceous aerosols. *Atmospheric Chemistry and Physics,* 6**,** 3131-3148.

Andrews, E., J. A. Ogren, S. Kinne & B. Samset (2017) Comparison of AOD, AAOD and column single scattering albedo from AERONET retrievals and in situ profiling measurements. *Atmospheric Chemistry and Physics,* 17**,** 6041-6072.

Bahadur, R., P. S. Praveen, Y. Y. Xu & V. Ramanathan (2012) Solar absorption by elemental and brown carbon determined from spectral observations. *Proceedings of the National Academy of Sciences of the United States of America,* 109**,** 17366-17371.

Bond, T. C. & R. W. Bergstrom (2006) Light absorption by carbonaceous particles: An investigative review. *Aerosol Science and Technology,* 40**,** 27-67.

Bond, T. C., S. J. Doherty, D. W. Fahey, P. M. Forster, T. Berntsen, B. J. DeAngelo, M. G. Flanner, S. Ghan, B. Karcher, D. Koch, S. Kinne, Y. Kondo, P. K. Quinn, M. C. Sarofim, M. G. Schultz, M. Schulz, C. Venkataraman, H. Zhang, S. Zhang, N. Bellouin, S. K. Guttikunda, P. K. Hopke, M. Z. Jacobson, J. W. Kaiser, Z. Klimont, U. Lohmann, J. P. Schwarz, D. Shindell, T. Storelvmo, S. G. Warren & C. S. Zender (2013) Bounding the role of black carbon in the climate system: A scientific assessment. *Journal of Geophysical Research-Atmospheres,* 118**,** 5380-5552.

Cappa, C. D., T. B. Onasch, P. Massoli, D. R. Worsnop, T. S. Bates, E. S. Cross, P. Davidovits, J. Hakala, K. L. Hayden, B. T. Jobson, K. R. Kolesar, D. A. Lack, B. M. Lerner, S. M. Li, D. Mellon, I. Nuaaman, J. S. Olfert, T. Petaja, P. K. Quinn, C. Song, R. Subramanian, E. J. Williams & R. A. Zaveri (2012) Radiative Absorption Enhancements Due to the Mixing State of Atmospheric Black Carbon. *Science,* 337**,** 1078-1081.

Chakrabarty, R. K., H. Moosmuller, L. W. A. Chen, K. Lewis, W. P. Arnott, C. Mazzoleni, M. K. Dubey, C. E. Wold, W. M. Hao & S. M. Kreidenweis (2010) Brown carbon in tar balls from smoldering biomass combustion. *Atmospheric Chemistry and Physics,* 10**,** 6363-6370.

Cheng, Y., K. B. He, Z. Y. Du, G. Engling, J. M. Liu, Y. L. Ma, M. Zheng & R. J. Weber (2016) The characteristics of brown carbon aerosol during winter in Beijing. *Atmospheric Environment,* 127**,** 355-364.

Cheng, Y., K. B. He, M. Zheng, F. K. Duan, Z. Y. Du, Y. L. Ma, J. H. Tan, F. M. Yang, J. M. Liu, X. L. Zhang, R. J. Weber, M. H. Bergin & A. G. Russell (2011) Mass absorption efficiency of elemental carbon and water-soluble organic carbon in Beijing, China. *Atmospheric Chemistry and Physics,* 11**,** 11497-11510.

Chow, J. C., L. W. A. Chen, J. G. Watson, D. H. Lowenthal, K. A. Magliano, K. Turkiewicz & D. E. Lehrman (2006) PM2.5 chemical composition and spatiotemporal variability during the California Regional PM10/PM2.5 Air Quality Study (CRPAQS). *Journal of Geophysical Research-Atmospheres,* 111.

Chow, J. C., J. G. Watson, L. C. Pritchett, W. R. Pierson, C. A. Frazier & R. G. Purcell (1993) THE DRI THERMAL OPTICAL REFLECTANCE CARBON ANALYSIS SYSTEM - DESCRIPTION, EVALUATION AND APPLICATIONS IN UNITED-STATES AIR-QUALITY STUDIES. *Atmospheric Environment Part a-General Topics,* 27**,** 1185-1201.

Chu, S. H., J. W. Paisie & B. W. L. Jang (2004) PM data analysis - a comparison of two urban areas: Fresno and Atlanta. *Atmospheric Environment,* 38**,** 3155-3164.

Chung, C. E., K. Lee & D. Mueller (2012a) Effect of internal mixture on black carbon radiative forcing. *Tellus Series B-Chemical and Physical Meteorology,* 64**,** 1-13.

Chung, C. E., V. Ramanathan & D. Decremer (2012b) Observationally constrained estimates of carbonaceous aerosol radiative forcing. *Proceedings of the National Academy of Sciences of the United States of America,* 109**,** 11624-11629.

Chung, S. H. & J. H. Seinfeld (2005) Climate response of direct radiative forcing of anthropogenic black carbon. *Journal of Geophysical Research-Atmospheres,* 110.

Collett, J. L., K. J. Hoag, D. E. Sherman, A. Bator & L. W. Richards (1999) Spatial and temporal variations in San Joaquin Valley fog chemistry. *Atmospheric Environment,* 33**,** 129-140.

Coniglio, M. C., K. L. Elmore, J. S. Kain, S. J. Weiss, M. Xue & M. L. Weisman (2010) Evaluation of WRF Model Output for Severe Weather Forecasting from the 2008 NOAA Hazardous Weather Testbed Spring Experiment. *Weather and Forecasting,* 25**,** 408-427.

Cooper, D. I. & W. E. Eichinger (1994) STRUCTURE OF THE ATMOSPHERE IN AN URBAN PLANETARY BOUNDARY-LAYER FROM LIDAR AND RADIOSONDE OBSERVATIONS. *Journal of Geophysical Research-Atmospheres,* 99**,** 22937-22948.

Corr, C. A., N. Krotkov, S. Madronich, J. R. Slusser, B. Holben, W. Gao, J. Flynn, B. Lefer & S. M. Kreidenweis (2009) Retrieval of aerosol single scattering albedo at ultraviolet wavelengths at the T1 site during MILAGRO. *Atmospheric Chemistry and Physics,* 9**,** 5813-5827.

Corrigan, C. E., G. C. Roberts, M. V. Ramana, D. Kim & V. Ramanathan (2008) Capturing vertical profiles of aerosols and black carbon over the Indian Ocean using autonomous unmanned aerial vehicles. *Atmospheric Chemistry and Physics,* 8**,** 737-747.

Davy, P. M., A. H. Tremper, E. M. G. Nicolosi, P. Quincey & G. W. Fuller (2017) Estimating particulate black carbon concentrations using two offline light absorption methods applied to four types of filter media. *Atmospheric Environment,* 152**,** 24-33.

Desyaterik, Y., Y. Sun, X. H. Shen, T. Y. Lee, X. F. Wang, T. Wang & J. L. Collett (2013) Speciation of "brown" carbon in cloud water impacted by agricultural biomass burning in eastern China. *Journal of Geophysical Research-Atmospheres,* 118**,** 7389-7399.

Devore, J. L. & K. N. Berk. *Modern mathematical statistics with applications*.

Docherty, K. S., E. A. Stone, I. M. Ulbrich, P. F. DeCarlo, D. C. Snyder, J. J. Schauer, R. E. Peltier, R. J. Weber, S. M. Murphy, J. H. Seinfeld, B. D. Grover, D. J. Eatough & J. L. Jimenez (2008) Apportionment of Primary and Secondary Organic Aerosols in Southern California during the 2005 Study of Organic Aerosols in Riverside (SOAR-1). *Environmental Science & Technology,* 42**,** 7655-7662.

Doran, C. (2007) "The T1-T2 study: evolution of aerosol properties downwind of Mexico City (vol 7, pg 1585, 2007). *Atmospheric Chemistry and Physics,* 7**,** 2197-2198.

Dubovik, O., B. Holben, T. F. Eck, A. Smirnov, Y. J. Kaufman, M. D. King, D. Tanre & I. Slutsker (2002) Variability of absorption and optical properties of key aerosol types observed in worldwide locations. *Journal of the Atmospheric Sciences,* 59**,** 590-608.

Dubovik, O. & M. D. King (2000) A flexible inversion algorithm for retrieval of aerosol optical properties from Sun and sky radiance measurements. *Journal of Geophysical Research-Atmospheres,* 105**,** 20673-20696.

Dubovik, O., A. Smirnov, B. N. Holben, M. D. King, Y. J. Kaufman, T. F. Eck & I. Slutsker

(2000) Accuracy assessments of aerosol optical properties retrieved from Aerosol Robotic Network (AERONET) Sun and sky radiance measurements. *Journal of Geophysical Research-Atmospheres,* 105**,** 9791-9806.

Esteve, A. R., J. A. Ogren, P. J. Sheridan, E. Andrews, B. N. Holben & M. P. Utrillas (2012) Sources of discrepancy between aerosol optical depth obtained from AERONET and in-situ aircraft profiles. *Atmospheric Chemistry and Physics,* 12**,** 2987-3003.

Fan, J., L. R. Leung, P. J. DeMott, J. M. Comstock, B. Singh, D. Rosenfeld, J. M. Tomlinson, A. White, K. A. Prather, P. Minnis, J. K. Ayers & Q. Min (2014) Aerosol impacts on California winter clouds and precipitation during CalWater 2011: local pollution versus long-range transported dust. *Atmospheric Chemistry and Physics,* 14**,** 81-101.

Favez, O., S. C. Alfaro, J. Sciare, H. Cachier & M. M. Abdelwahab (2009) Ambient measurements of light-absorption by agricultural waste burning organic aerosols. *Journal of Aerosol Science,* 40**,** 613-620.

Feng, Y., V. Ramanathan & V. R. Kotamarthi (2013) Brown carbon: a significant atmospheric absorber of solar radiation? *Atmospheric Chemistry and Physics,* 13**,** 8607-8621.

Fialho, P., M. C. Freitas, F. Barata, B. Vieira, A. D. A. Hansen & R. E. Honrath (2006) The Aethalometer calibration and determination of iron concentration in dust aerosols. *Journal of Aerosol Science,* 37**,** 1497-1506.

Forrister, H., J. Liu, E. Scheuer, J. Dibb, L. Ziemba, K. L. Thornhill, B. Anderson, G. Diskin, A. E. Perring, J. P. Schwarz, P. Campuzano-Jost, D. A. Day, B. B. Palm, J. L. Jimenez, A. Nenes & R. J. Weber (2015) Evolution of brown carbon in wildfire plumes. *Geophysical Research Letters,* 42**,** 4623-4630.

Galchen, T., M. Xu & W. L. Eberhard (1992) ESTIMATIONS OF ATMOSPHERIC BOUNDARY-LAYER FLUXES AND OTHER TURBULENCE PARAMETERS FROM DOPPLER LIDAR DATA. *Journal of Geophysical Research-Atmospheres,* 97**,** 18409-18423.

Ge, X., A. Setyan, Y. Sun & Q. Zhang (2012) Primary and secondary organic aerosols in Fresno, California during wintertime: Results from high resolution aerosol mass spectrometry. *Journal of Geophysical Research-Atmospheres,* 117.

Gobbi, G. P., F. Barnaba & L. Ammannato (2004) The vertical distribution of aerosols, Saharan dust and cirrus clouds in Rome (Italy) in the year 2001. *Atmospheric Chemistry and Physics,* 4**,** 351-359.

Gorin, C. A., J. L. Collett, Jr. & P. Herckes (2006) Wood smoke contribution to winter aerosol in Fresno, CA. *Journal of the Air & Waste Management Association,* 56**,** 1584-1590.

Gyawali, M., W. P. Arnott, K. Lewis & H. Moosmuller (2009) In situ aerosol optics in Reno, NV, USA during and after the summer 2008 California wildfires and the influence of absorbing and non-absorbing organic coatings on spectral light absorption. *Atmospheric Chemistry and Physics,* 9**,** 8007-8015.

Hariharan, P. 2007. *Basics of Interferometry, 2nd Edition.*

Hayes, P. L., A. M. Ortega, M. J. Cubison, K. D. Froyd, Y. Zhao, S. S. Cliff, W. W. Hu, D. W. Toohey, J. H. Flynn, B. L. Lefer, N. Grossberg, S. Alvarez, B. Rappenglueck, J. W. Taylor, J. D. Allan, J. S. Holloway, J. B. Gilman, W. C. Kuster, J. A. De Gouw, P. Massoli, X. Zhang, J. Liu, R. J. Weber, A. L. Corrigan, L. M. Russell, G. Isaacman, D. R. Worton, N. M. Kreisberg, A. H. Goldstein, R. Thalman, E. M. Waxman, R. Volkamer, Y. H. Lin, J. D. Surratt, T. E. Kleindienst, J. H. Offenberg, S. Dusanter, S. Griffith, P. S. Stevens, J. Brioude, W. M. Angevine & J. L. Jimenez (2013) Organic aerosol composition and sources in Pasadena, California, during the 2010 CalNex campaign. *Journal of Geophysical Research-Atmospheres,* 118**,** 9233-9257.

Haywood, J., P. Francis, O. Dubovik, M. Glew & B. Holben (2003) Comparison of aerosol size distributions, radiative properties, and optical depths determined by aircraft observations and Sun photometers during SAFARI 2000. *Journal of Geophysical Research-Atmospheres,* 108.

Healy, R. M., J. M. Wang, C. H. Jeong, A. K. Y. Lee, M. D. Willis, E. Jaroudi, N. Zimmerman, N. Hilker, M. Murphy, S. Eckhardt, A. Stohl, J. P. D. Abbatt, J. C. Wenger & G. J. Evans (2015) Light-absorbing properties of ambient black carbon and brown carbon from fossil fuel and biomass burning sources. *Journal of Geophysical Research-Atmospheres,* 120**,** 6619-6633.

Herckes, P., J. A. Leenheer & J. L. Collett, Jr. (2007) Comprehensive characterization of atmospheric organic matter in Fresno, California fog water. *Environmental Science & Technology,* 41**,** 393-399.

Hodnebrog, O., G. Myhre, P. M. Forster, J. Sillmann & B. H. Samset (2016) Local biomass burning is a dominant cause of the observed precipitation reduction in southern Africa. *Nature Communications,* 7.

Hoffer, A., A. Gelencser, P. Guyon, G. Kiss, O. Schmid, G. P. Frank, P. Artaxo & M. O.

Andreae (2006) Optical properties of humic-like substances (HULIS) in biomass-burning aerosols. *Atmospheric Chemistry and Physics,* 6**,** 3563-3570.

Hoffer, A., A. Toth, I. Nyiro-Kosa, M. Posfai & A. Gelencser (2016) Light absorption properties of laboratory-generated tar ball particles. *Atmospheric Chemistry and Physics,* 16**,** 239-246.

Holben, B. N., T. F. Eck, I. Slutsker, D. Tanre, J. P. Buis, A. Setzer, E. Vermote, J. A. Reagan, Y. J. Kaufman, T. Nakajima, F. Lavenu, I. Jankowiak & A. Smirnov (1998) AERONET - A federated instrument network and data archive for aerosol characterization. *Remote Sensing of Environment,* 66**,** 1-16.

Holben, B. N., D. Tanre, A. Smirnov, T. F. Eck, I. Slutsker, N. Abuhassan, W. W. Newcomb, J. S. Schafer, B. Chatenet, F. Lavenu, Y. J. Kaufman, J. V. Castle, A. Setzer, B. Markham, D. Clark, R. Frouin, R. Halthore, A. Karneli, N. T. O'Neill, C. Pietras, R. T. Pinker, K. Voss & G. Zibordi (2001) An emerging ground-based aerosol climatology: Aerosol optical depth from AERONET. *Journal of Geophysical Research-Atmospheres,* 106**,** 12067-12097.

Hu, J. L., H. L. Zhang, S. H. Chen, C. Wiedinmyer, F. Vandenberghe, Q. Ying & M. J. Kleeman (2014) Predicting Primary PM2.5 and PM0.1 Trace Composition for Epidemiological Studies in California. *Environmental Science & Technology,* 48**,** 4971-4979.

Jacobson, M. Z. (2001) Strong radiative heating due to the mixing state of black carbon in atmospheric aerosols. *Nature,* 409**,** 695-697.

Jo, D. S., R. J. Park, S. Lee, S.-W. Kim & X. Zhang (2016) A global simulation of brown carbon: implications for photochemistry and direct radiative effect. *Atmospheric Chemistry and Physics,* 16**,** 3413-3432.

Johnson, B. T., S. Christopher, J. M. Haywood, S. R. Osborne, S. McFarlane, C. Hsu, C. Salustro & R. Kahn (2009) Measurements of aerosol properties from aircraft, satellite and ground-based remote sensing: A case-study from the Dust and Biomass-burning Experiment (DABEX). *Quarterly Journal of the Royal Meteorological Society,* 135**,** 922-934.

Kirchstetter, T. W., T. Novakov & P. V. Hobbs (2004) Evidence that the spectral dependence of light absorption by aerosols is affected by organic carbon. *Journal of Geophysical Research-Atmospheres,* 109.

Knox, A., G. J. Evans, J. R. Brook, X. Yao, C. H. Jeong, K. J. Godri, K. Sabaliauskas & J. G. Slowik (2009) Mass Absorption Cross-Section of Ambient Black Carbon Aerosol in Relation to Chemical Age. *Aerosol Science and Technology,* 43**,** 522-

532.

Koch, D., M. Schulz, S. Kinne, C. McNaughton, J. R. Spackman, Y. Balkanski, S. Bauer, T. Berntsen, T. C. Bond, O. Boucher, M. Chin, A. Clarke, N. De Luca, F. Dentener, T. Diehl, O. Dubovik, R. Easter, D. W. Fahey, J. Feichter, D. Fillmore, S. Freitag, S. Ghan, P. Ginoux, S. Gong, L. Horowitz, T. Iversen, A. Kirkevag, Z. Klimont, Y. Kondo, M. Krol, X. Liu, R. Miller, V. Montanaro, N. Moteki, G. Myhre, J. E. Penner, J. Perlwitz, G. Pitari, S. Reddy, L. Sahu, H. Sakamoto, G. Schuster, J. P. Schwarz, O. Seland, P. Stier, N. Takegawa, T. Takemura, C. Textor, J. A. van Aardenne & Y. Zhao (2009) Evaluation of black carbon estimations in global aerosol models. *Atmospheric Chemistry and Physics,* 9**,** 9001-9026.

Kotchenruther, R. A., P. V. Hobbs & D. A. Hegg (1999) Humidification factors for atmospheric aerosols off the mid-Atlantic coast of the United States. *Journal of Geophysical Research-Atmospheres,* 104**,** 2239-2251.

Lack, D. A. & J. M. Langridge (2013) On the attribution of black and brown carbon light absorption using the Angstrom exponent. *Atmospheric Chemistry and Physics,* 13**,** 10535-10543.

Lack, D. A., J. M. Langridge, R. Bahreini, C. D. Cappa, A. M. Middlebrook & J. P. Schwarz (2012) Brown carbon and internal mixing in biomass burning particles. *Proceedings of the National Academy of Sciences of the United States of America,* 109**,** 14802-14807.

Lack, D. A., P. K. Quinn, P. Massoli, T. S. Bates, D. Coffman, D. S. Covert, B. Sierau, S. Tucker, T. Baynard, E. Lovejoy, D. M. Murphy & A. R. Ravishankara (2009) Relative humidity dependence of light absorption by mineral dust after long-range atmospheric transport from the Sahara. *Geophysical Research Letters,* 36.

Leahy, L. V., T. L. Anderson, T. F. Eck & R. W. Bergstrom (2007) A synthesis of single scattering albedo of biomass burning aerosol over southern Africa during SAFARI 2000. *Geophysical Research Letters,* 34.

Lee, H. J., P. K. Aiona, A. Laskin, J. Laskin & S. A. Nizkorodov (2014) Effect of Solar Radiation on the Optical Properties and Molecular Composition of Laboratory Proxies of Atmospheric Brown Carbon. *Environmental Science & Technology,* 48**,** 10217-10226.

Li, Z. Q., J. P. Guo, A. J. Ding, H. Liao, J. J. Liu, Y. L. Sun, T. J. Wang, H. W. Xue, H. S. Zhang & B. Zhu (2017) Aerosol and boundary-layer interactions and impact on air quality. *National Science Review,* 4**,** 810-833.

Lin, G. X., J. E. Penner, M. G. Flanner, S. Sillman, L. Xu & C. Zhou (2014) Radiative forcing of organic aerosol in the atmosphere and on snow: Effects of SOA and brown carbon. *Journal of Geophysical Research-Atmospheres,* 119**,** 7453-7476.

Liu, D., J. Whitehead, M. R. Alfarra, E. Reyes-Villegas, D. V. Spracklen, C. L. Reddington, S. Kong, P. I. Williams, Y.-C. Ting, S. Haslett, J. W. Taylor, M. J. Flynn, W. T. Morgan, G. McFiggans, H. Coe & J. D. Allan (2017) Black-carbon absorption enhancement in the atmosphere determined by particle mixing state. *Nature Geoscience,* 10**,** 184-U132.

Liu, J., M. Bergin, H. Guo, L. King, N. Kotra, E. Edgerton & R. J. Weber (2013) Size-resolved measurements of brown carbon in water and methanol extracts and estimates of their contribution to ambient fine-particle light absorption. *Atmospheric Chemistry and Physics,* 13**,** 12389-12404.

Liu, J., E. Scheuer, J. Dibb, G. S. Diskin, L. D. Ziemba, K. L. Thornhill, B. E. Anderson, A. Wisthaler, T. Mikoviny, J. J. Devi, M. Bergin, A. E. Perring, M. Z. Markovic, J. P. Schwarz, P. Campuzano-Jost, D. A. Day, J. L. Jimenez & R. J. Weber (2015a) Brown carbon aerosol in the North American continental troposphere: sources, abundance, and radiative forcing. *Atmospheric Chemistry and Physics,* 15**,** 7841-7858.

Liu, P. F., C. S. Zhao, Q. Zhang, Z. Z. Deng, M. Y. Huang, X. C. Ma & X. X. Tie (2009) Aircraft study of aerosol vertical distributions over Beijing and their optical properties. *Tellus Series B-Chemical and Physical Meteorology,* 61**,** 756-767.

Liu, S., A. C. Aiken, K. Gorkowski, M. K. Dubey, C. D. Cappa, L. R. Williams, S. C. Herndon, P. Massoli, E. C. Fortner, P. S. Chhabra, W. A. Brooks, T. B. Onasch, J. T. Jayne, D. R. Worsnop, S. China, N. Sharma, C. Mazzoleni, L. Xu, N. L. Ng, D. Liu, J. D. Allan, J. D. Lee, Z. L. Fleming, C. Mohr, P. Zotter, S. Szidat & A. S. H. Prevot (2015b) Enhanced light absorption by mixed source black and brown carbon particles in UK winter. *Nature Communications,* 6.

Lurmann, F. W., S. G. Brown, M. C. McCarthy & P. T. Roberts (2006) Processes influencing secondary aerosol formation in the San Joaquin Valley during winter. *Journal of the Air & Waste Management Association,* 56**,** 1679-1693.

Magi, B. I., P. V. Hobbs, T. W. Kirchstetter, T. Novakov, D. A. Hegg, S. Gao, J. Redemann & B. Schmid (2005) Aerosol properties and chemical apportionment of aerosol optical depth at locations off the US east coast in July and August 2001. *Journal of the Atmospheric Sciences,* 62**,** 919-933.

Mallet, M., V. Pont, C. Liousse, L. Gomes, J. Pelon, S. Osborne, J. Haywood, J. C.

Roger, P. Dubuisson, A. Mariscal, V. Thouret & P. Goloub (2008) Aerosol direct radiative forcing over Djougou (northern Benin) during the African Monsoon Multidisciplinary Analysis dry season experiment (Special Observation Period-0). *Journal of Geophysical Research-Atmospheres,* 113.

Mallet, M., R. Van Dingenen, J. C. Roger, S. Despiau & H. Cachier (2005) In situ airborne measurements of aerosol optical properties during photochemical pollution events. *Journal of Geophysical Research-Atmospheres,* 110.

Matthes, F. C. (2008) Climate change 2007. The physical science basis, impacts, adaptation and vulnerability mitigation of climate change. *Internationale Politik,* 63**,** 130-132.

Michelsen, H. A. (2003) Understanding and predicting the temporal response of laser-induced incandescence from carbonaceous particles. *Journal of Chemical Physics,* 118**,** 7012-7045.

Molders, N. & G. Kramm (2010) A case study on wintertime inversions in Interior Alaska with WRF. *Atmospheric Research,* 95**,** 314-332.

Moosmueller, H., R. K. Chakrabarty, K. M. Ehlers & W. P. Arnott (2011) Absorption Angstrom coefficient, brown carbon, and aerosols: basic concepts, bulk matter, and spherical particles. *Atmospheric Chemistry and Physics,* 11**,** 1217-1225.

Moosmuller, H., R. K. Chakrabarty & W. P. Arnott (2009) Aerosol light absorption and its measurement: A review. *Journal of Quantitative Spectroscopy & Radiative Transfer,* 110**,** 844-878.

Myhre, G., B. H. Samset, M. Schulz, Y. Balkanski, S. Bauer, T. K. Berntsen, H. Bian, N. Bellouin, M. Chin, T. Diehl, R. C. Easter, J. Feichter, S. J. Ghan, D. Hauglustaine, T. Iversen, S. Kinne, A. Kirkevag, J. F. Lamarque, G. Lin, X. Liu, M. T. Lund, G. Luo, X. Ma, T. van Noije, J. E. Penner, P. J. Rasch, A. Ruiz, O. Seland, R. B. Skeie, P. Stier, T. Takemura, K. Tsigaridis, P. Wang, Z. Wang, L. Xu, H. Yu, F. Yu, J. H. Yoon, K. Zhang, H. Zhang & C. Zhou (2013) Radiative forcing of the direct aerosol effect from AeroCom Phase II simulations. *Atmospheric Chemistry and Physics,* 13**,** 1853-1877.

Nakayama, T., Y. Ikeda, Y. Sawada, Y. Setoguchi, S. Ogawa, K. Kawana, M. Mochida, F. Ikemori, K. Matsumoto & Y. Matsumi (2014) Properties of light-absorbing aerosols in the Nagoya urban area, Japan, in August 2011 and January 2012: Contributions of brown carbon and lensing effect. *Journal of Geophysical Research-Atmospheres,* 119**,** 12721-12739.

Ngo, M. A., K. E. Pinkerton, S. Freeland, M. Geller, W. Ham, S. Cliff, L. E. Hopkins, M.

J. Kleeman, U. P. Kodavanti, E. Meharg, L. Plummer, J. J. Recendez, M. B. Schenker, C. Sioutas, S. Smiley-Jewell, C. Haas, J. Gutstein & A. S. Wexler (2010) Airborne particles in the San Joaquin Valley may affect human health. *California Agriculture,* 64**,** 12-16.

Osborne, S. R., B. T. Johnson, J. M. Haywood, A. J. Baran, M. A. J. Harrison & C. L. McConnell (2008) Physical and optical properties of mineral dust aerosol during the Dust and Biomass-burning Experiment. *Journal of Geophysical Research-Atmospheres,* 113.

Petzold, A. & M. Schonlinner (2004) Multi-angle absorption photometry - a new method for the measurement of aerosol light absorption and atmospheric black carbon. *Journal of Aerosol Science,* 35**,** 421-441.

Pope, C. A., III & D. W. Dockery (2006) Health effects of fine particulate air pollution: Lines that connect. *Journal of the Air & Waste Management Association,* 56**,** 709-742.

Pratt, K. A., P. J. DeMott, J. R. French, Z. Wang, D. L. Westphal, A. J. Heymsfield, C. H. Twohy, A. J. Prenni & K. A. Prather (2009) In situ detection of biological particles in cloud ice-crystals. *Nature Geoscience,* 2**,** 397-400.

Pringle, K. J., H. Tost, A. Pozzer, U. Poschl & J. Lelieveld (2010) Global distribution of the effective aerosol hygroscopicity parameter for CCN activation. *Atmospheric Chemistry and Physics,* 10**,** 5241-5255.

Pusede, S. E., K. C. Duffey, A. A. Shusterman, A. Saleh, J. L. Laughner, P. J. Wooldridge, Q. Zhang, C. L. Parworth, H. Kim, S. L. Capps, L. C. Valin, C. D. Cappa, A. Fried, J. Walega, J. B. Nowak, A. J. Weinheimer, R. M. Hoff, T. A. Berkoff, A. J. Beyersdorf, J. Olson, J. H. Crawford & R. C. Cohen (2016) On the effectiveness of nitrogen oxide reductions as a control over ammonium nitrate aerosol. *Atmospheric Chemistry and Physics,* 16**,** 2575-2596.

Ramanathan, V. & G. Carmichael (2008) Global and regional climate changes due to black carbon. *Nature Geoscience,* 1**,** 221-227.

Russell, P. B., R. W. Bergstrom, Y. Shinozuka, A. D. Clarke, P. F. DeCarlo, J. L. Jimenez, J. M. Livingston, J. Redemann, O. Dubovik & A. Strawa (2010) Absorption Angstrom Exponent in AERONET and related data as an indicator of aerosol composition. *Atmospheric Chemistry and Physics,* 10**,** 1155-1169.

Saathoff, H., O. Mohler, U. Schurath, S. Kamm, B. Dippel & D. Mihelcic (2003) The AIDA soot aerosol characterisation campaign 1999. *Journal of Aerosol Science,* 34**,** 1277-1296.

Saleh, R., C. J. Hennigan, G. R. McMeeking, W. K. Chuang, E. S. Robinson, H. Coe, N. M. Donahue & A. L. Robinson (2013) Absorptivity of brown carbon in fresh and photo-chemically aged biomass-burning emissions. *Atmospheric Chemistry and Physics,* 13**,** 7683-7693.

Saleh, R., E. S. Robinson, D. S. Tkacik, A. T. Ahern, S. Liu, A. C. Aiken, R. C. Sullivan, A. A. Presto, M. K. Dubey, R. J. Yokelson, N. M. Donahue & A. L. Robinson (2014) Brownness of organics in aerosols from biomass burning linked to their black carbon content. *Nature Geoscience,* 7**,** 647-650.

Schafer, J. S., T. F. Eck, B. N. Holben, K. L. Thornhill, B. E. Anderson, A. Sinyuk, D. M. Giles, E. L. Winstead, L. D. Ziemba, A. J. Beyersdorf, P. R. Kenny, A. Smirnov & I. Slutsker (2014) Intercomparison of aerosol single-scattering albedo derived from AERONET surface radiometers and LARGE in situ aircraft profiles during the 2011 DRAGON-MD and DISCOVER-AQ experiments. *Journal of Geophysical Research-Atmospheres,* 119**,** 7439-7452.

Schnaiter, M., H. Horvath, O. Mohler, K. H. Naumann, H. Saathoff & O. W. Schock (2003) UV-VIS-NIR spectral optical properties of soot and soot-containing aerosols. *Journal of Aerosol Science,* 34**,** 1421-1444.

Schnaiter, M., C. Linke, O. Mohler, K. H. Naumann, H. Saathoff, R. Wagner, U. Schurath & B. Wehner (2005) Absorption amplification of black carbon internally mixed with secondary organic aerosol. *Journal of Geophysical Research-Atmospheres,* 110.

Shen, G. F., S. Tao, Y. C. Chen, Y. Y. Zhang, S. Y. Wei, M. Xue, B. Wang, R. Wang, Y. Lu, W. Li, H. Z. Shen, Y. Huang & H. Chen (2013) Emission Characteristics for Polycyclic Aromatic Hydrocarbons from Solid Fuels Burned in Domestic Stoves in Rural China. *Environmental Science & Technology,* 47**,** 14485-14494.

Shiraiwa, M., Y. Kondo, T. Iwamoto & K. Kita (2010) Amplification of Light Absorption of Black Carbon by Organic Coating. *Aerosol Science and Technology,* 44**,** 46-54.

Singh, A., P. Rajput, D. Sharma, M. M. Sarin & D. Singh (2014) Black Carbon and Elemental Carbon from Postharvest Agricultural-Waste Burning Emissions in the Indo-Gangetic Plain. *Advances in Meteorology*.

Skupin, A., A. Ansmann, R. Engelmann, P. Seifert & T. Muller (2016) Four-year long-path monitoring of ambient aerosol extinction at a central European urban site: dependence on relative humidity. *Atmospheric Chemistry and Physics,* 16**,** 1863-1876.

Slowik, J. G., E. S. Cross, J.-H. Han, P. Davidovits, T. B. Onasch, J. T. Jayne, L. R. WilliamS, M. R. Canagaratna, D. R. Worsnop, R. K. Chakrabarty, H. Moosmueller, W. P. Arnott, J. P. Schwarz, R.-S. Gao, D. W. Fahey, G. L. Kok & A. Petzold (2007) An inter-comparison of instruments measuring black carbon content of soot particles. *Aerosol Science and Technology,* 41**,** 295-314.

Smirnov, A., B. N. Holben, T. F. Eck, O. Dubovik & I. Slutsker (2000) Cloud-screening and quality control algorithms for the AERONET database. *Remote Sensing of Environment,* 73**,** 337-349.

Stocker, T. & Intergovernmental Panel on Climate Change. Working Group I. *Climate change 2013 : the physical science basis : Working Group I contribution to the Fifth assessment report of the Intergovernmental Panel on Climate Change*.

Strawa, A. W., R. Castaneda, T. Owano, D. S. Baer & B. A. Paldus (2003) The measurement of aerosol optical properties using continuous wave cavity ring-down techniques. *Journal of Atmospheric and Oceanic Technology,* 20**,** 454-465.

Sullivan, A. P. & R. J. Weber (2006) Chemical characterization of the ambient organic aerosol soluble in water: 1. Isolation of hydrophobic and hydrophilic fractions with a XAD-8 resin. *Journal of Geophysical Research-Atmospheres,* 111.

Tam, A. C. (1986) APPLICATIONS OF PHOTOACOUSTIC SENSING TECHNIQUES. *Reviews of Modern Physics,* 58**,** 381-431.

Turkiewicz, K., K. Magliano & T. Najita (2006) Comparison of two winter air quality episodes during the California Regional Particulate Air Quality Study. *Journal of the Air & Waste Management Association,* 56**,** 467-473.

Virkkula, A., N. C. Ahlquist, D. S. Covert, P. J. Sheridan, W. P. Arnott & J. A. Ogren (2005) A three-wavelength optical extinction cell for measuring aerosol light extinction and its application to determining light absorption coefficient. *Aerosol Science and Technology,* 39**,** 52-67.

Wang, Q. Q., D. J. Jacob, J. R. Spackman, A. E. Perring, J. P. Schwarz, N. Moteki, E. A. Marais, C. Ge, J. Wang & S. R. H. Barrett (2014a) Global budget and radiative forcing of black carbon aerosol: Constraints from pole-to-pole (HIPPO) observations across the Pacific. *Journal of Geophysical Research-Atmospheres,* 119**,** 195-206.

Wang, Q. Y., R. J. Huang, J. J. Cao, Y. M. Han, G. H. Wang, G. H. Li, Y. C. Wang, W. T. Dai, R. J. Zhang & Y. Q. Zhou (2014b) Mixing State of Black Carbon Aerosol

in a Heavily Polluted Urban Area of China: Implications for Light Absorption Enhancement. *Aerosol Science and Technology,* 48**,** 689-697.

Wang, R., E. Andrews, Y. Balkanski, O. Boucher, G. Myhre, B. H. Samset, M. Schulz, G. L. Schuster, M. Valari & S. Tao (2018) Spatial Representativeness Error in the Ground-Level Observation Networks for Black Carbon Radiation Absorption. *Geophysical Research Letters,* 45**,** 2106-2114.

Wang, R., Y. Balkanski, O. Boucher, P. Ciais, G. L. Schuster, F. Chevallier, B. H. Samset, J. Liu, S. Piao, M. Valari & S. Tao (2016a) Estimation of global black carbon direct radiative forcing and its uncertainty constrained by observations. *Journal of Geophysical Research-Atmospheres,* 121**,** 5948-5971.

Wang, X., C. L. Heald, D. A. Ridley, J. P. Schwarz, J. R. Spackman, A. E. Perring, H. Coe, D. Liu & A. D. Clarke (2014c) Exploiting simultaneous observational constraints on mass and absorption to estimate the global direct radiative forcing of black carbon and brown carbon. *Atmospheric Chemistry and Physics,* 14**,** 10989-11010.

Wang, X., C. L. Heald, A. J. Sedlacek, S. S. de Sa, S. T. Martin, M. L. Alexander, T. B. Watson, A. C. Aiken, S. R. Springston & P. Artaxo (2016b) Deriving brown carbon from multiwavelength absorption measurements: method and application to AERONET and Aethalometer observations. *Atmospheric Chemistry and Physics,* 16**,** 12733-12752.

Watson, J. G. (2002) Visibility: Science and regulation. *Journal of the Air & Waste Management Association,* 52**,** 628-713.

Winker, D. M., J. L. Tackett, B. J. Getzewich, Z. Liu, M. A. Vaughan & R. R. Rogers (2013) The global 3-D distribution of tropospheric aerosols as characterized by CALIOP. *Atmospheric Chemistry and Physics,* 13**,** 3345-3361.

Wu, G. M., Z. Y. Cong, S. C. Kang, K. Kawamura, P. Q. Fu, Y. L. Zhang, X. Wan, S. P. Gao & B. Liu (2016) Brown carbon in the cryosphere: Current knowledge and perspective. *Advances in Climate Change Research,* 7**,** 82-89.

Xu, B. Q., J. J. Cao, J. Hansen, T. D. Yao, D. R. Joswia, N. L. Wang, G. J. Wu, M. Wang, H. B. Zhao, W. Yang, X. Q. Liu & J. Q. He (2009) Black soot and the survival of Tibetan glaciers. *Proceedings of the National Academy of Sciences of the United States of America,* 106**,** 22114-22118.

Yang, M., S. G. Howell, J. Zhuang & B. J. Huebert (2009) Attribution of aerosol light absorption to black carbon, brown carbon, and dust in China - interpretations of atmospheric measurements during EAST-AIRE. *Atmospheric Chemistry and*

Physics, 9**,** 2035-2050.

Young, D. E., H. Kim, C. Parworth, S. Zhou, X. L. Zhang, C. D. Cappa, R. Seco, S. Kim & Q. Zhang (2016) Influences of emission sources and meteorology on aerosol chemistry in a polluted urban environment: results from DISCOVER-AQ California. *Atmospheric Chemistry and Physics,* 16**,** 5427-5451.

Zhang, Q., J. L. Jimenez, M. R. Canagaratna, I. M. Ulbrich, N. L. Ng, D. R. Worsnop & Y. Sun (2011a) Understanding atmospheric organic aerosols via factor analysis of aerosol mass spectrometry: a review. *Analytical and Bioanalytical Chemistry,* 401**,** 3045-3067.

Zhang, X. L., H. Kim, C. L. Parworth, D. E. Young, Q. Zhang, A. R. Metcalf & C. D. Cappa (2016) Optical Properties of Wintertime Aerosols from Residential Wood Burning in Fresno, CA: Results from DISCOVER-AQ 2013. *Environmental Science & Technology,* 50**,** 1681-1690.

Zhang, X. L., Y. H. Lin, J. D. Surratt & R. J. Weber (2013) Sources, Composition and Absorption Angstrom Exponent of Light-absorbing Organic Components in Aerosol Extracts from the Los Angeles Basin. *Environmental Science & Technology,* 47**,** 3685-3693.

Zhang, X. L., Y. H. Lin, J. D. Surratt, P. Zotter, A. S. H. Prevot & R. J. Weber (2011b) Light-absorbing soluble organic aerosol in Los Angeles and Atlanta: A contrast in secondary organic aerosol. *Geophysical Research Letters,* 38.

Zhao, R., A. K. Y. Lee, L. Huang, X. Li, F. Yang & J. P. D. Abbatt (2015) Photochemical processing of aqueous atmospheric brown carbon. *Atmospheric Chemistry and Physics,* 15**,** 6087-6100.